Supporting Information for

Hydrogen Addition to (pincer)Ir^{I}(CO) Complexes: The Importance of Steric and Electronic Factors

Jonathan M. Goldberg, Sophia D. T. Cherry, Louise M. Guard, Werner Kaminsky, Karen I. Goldberg,* D. Michael Heinekey*

Department of Chemistry, University of Washington, Seattle, Washington 98195-1700, United States

Table of Contents

S2 General Considerations

S2 Synthesis and Characterization of Compounds

S15 Experimental Procedures

S28 pK_a Determination of $[^{(tBu)4}(POCOP)Ir(CO)(H)]^+$

S30 Hydrogen Pressurization System

S39 X-ray Crystallography

S43 References

General Considerations

All experiments and manipulations were performed using standard Schlenk techniques under an argon atmosphere or in an argon or nitrogen filled glove box. Glassware and diatomaceous earth were dried in an oven maintained at 140 °C for at least 24 h. Deuterated solvents were dried over calcium hydride or molecular sieves (CD_2Cl_2, THF-d_8, and C_6D_6) or sodium/benzophenone (toluene-d_8) and vacuum transferred prior to use. Protio solvents were passed through columns of activated alumina and molecular sieves. All other reagents were used as received. ^{1}H NMR spectra were referenced to residual protio solvents: dichloromethane (5.32 ppm), THF (1.79 ppm), toluene (2.09 ppm), and benzene (7.16 ppm). ^{13}C NMR shifts were referenced to solvent signals: benzene (128.06 ppm), dichloromethane (54.00 ppm) and THF (26.19 ppm). ^{31}P NMR shifts were referenced to an 85% H_3PO_4 external standard (0 ppm). Infrared spectra were recorded on a Bruker Tensor 27 FTIR instrument. NMR spectra were recorded on either a Bruker AV-700, AV-500, DRX-500, or AV-300 NMR instrument. X-ray data was collected at -173°C on a Bruker APEX II single crystal X-ray diffractometer, Mo-radiation. Elemental analysis was performed under air-free conditions at the CENTC facility at the University of Rochester or Atlantic Microlabs. Anhydrous *p*-toluenesulfonic acid was prepared by heating the monohydrate under vacuum at 50°C. $^{(tBu)4}$(POCOP)Ir(CO) and $^{(tBu)4}$(POCOP)Ir(H)$_2$,[1] $^{(iPr)4}$(POCOP)Ir(CO)(H)(Cl),[2] and [Hlut]X and [Hpyr]X (for X = BF_4 or $BArF_{20}$)[3] were synthesized according to published procedures.

Synthesis and Characterization of Compounds

*Improved Synthesis of [$^{(tBu)4}$(POCOP)Ir(CO)(H)]$BArF_{20}$ (**3-$BArF_{20}$**).* In air, HCl/Et_2O (0.6 mL of 2.0 M solution) was added to a solution of $^{(tBu)4}$(POCOP)Ir(CO) (**1**) (32.3 mg, 0.0523 mmol) in C_6H_6 giving a colorless solution. Upon lyophilization, a white solid was obtained. In a nitrogen-filled glovebox, the white solid was combined with $KBArF_{20}$ (36 mg, 0.050 mmol) and dissolved in CH_2Cl_2 (5 mL) resulting in an orange solution and formation of a white precipitate. After sitting at room temperature for 8 h, the solution was filtered through a pad of diatomaceous earth and concentrated to 1 mL. The solution was layered with pentane (9 mL) and stored at -30 °C, yielding orange crystals. The mother liquor was removed and the orange solid was washed with pentane (3 mL). The solid was dried under vacuum giving a pale orange powder; yield: 52 mg (0.040 mmol, 80%). ^{1}H NMR (CD_2Cl_2, 300.10 MHz, 25 °C): δ 7.37 (t, $^3J_{HH}$ = 8.1 Hz, 1H; Ar-*H*), 6.95 (d, $^3J_{HH}$ = 8.1 Hz, 2H; Ar-*H*), 1.37 (m, 36H; P-C(C*H*$_3$)$_3$), -35.76 (t, $^2J_{PH}$ = 10.4 Hz, 1H; Ir-*H*). ^{31}P{^{1}H} NMR (CD_2Cl_2, 121.51 MHz, 22 °C): δ 191.8 (s).

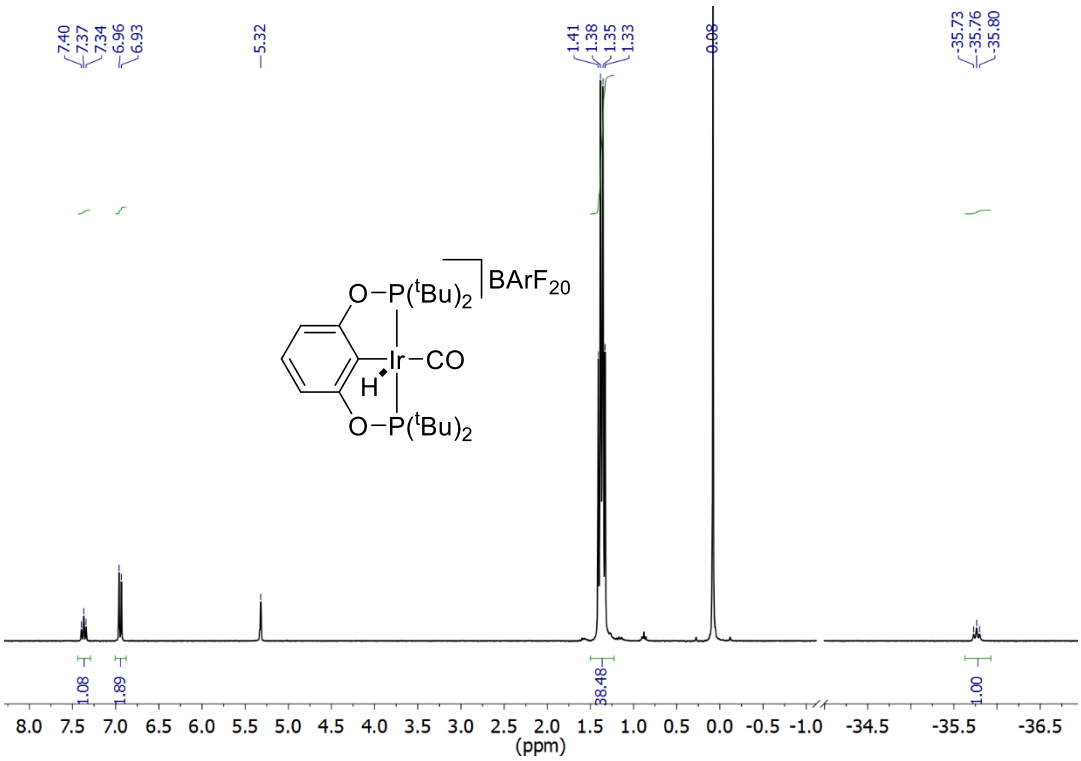

Figure S1. ^{1}H NMR spectrum of [$^{(tBu)4}$(POCOP)Ir(CO)(H)]$BArF_{20}$ (**3-BArF$_{20}$**) in CD_2Cl_2.

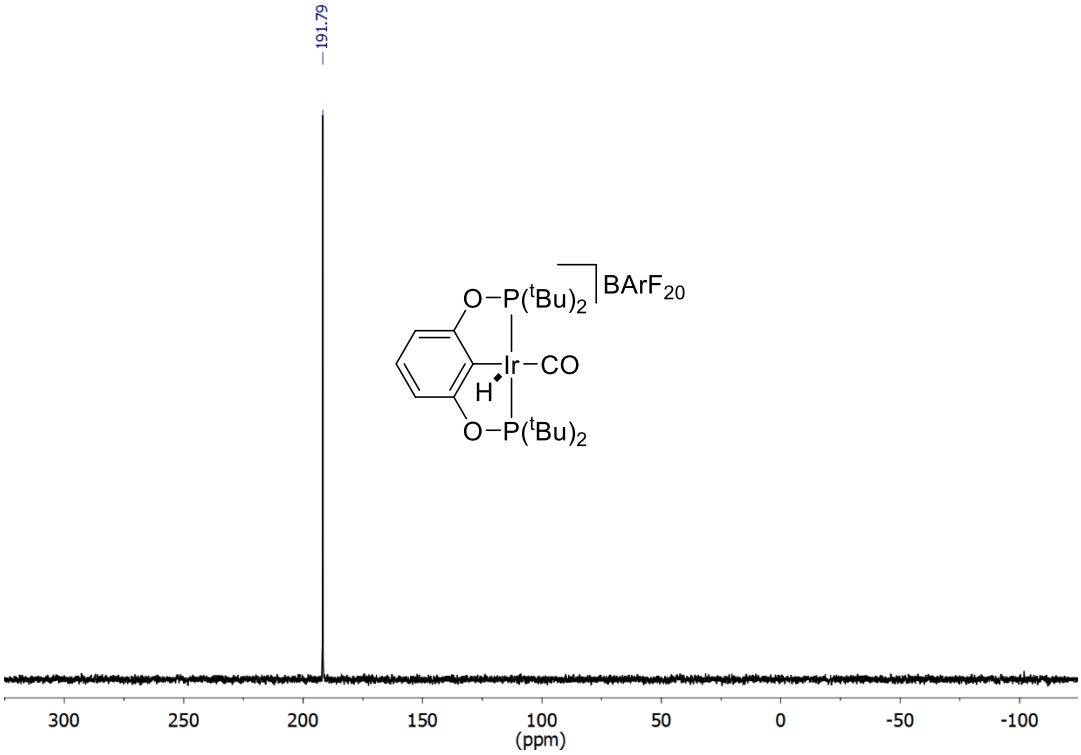

Figure S2. $^{31}P\{^{1}H\}$ NMR spectrum of [$^{(tBu)4}$(POCOP)Ir(CO)(H)]$BArF_{20}$ (**3-BArF$_{20}$**) in CD_2Cl_2.

Synthesis of trans-$^{(iPr)4}$*(POCOP)Ir(CO)(H)*$_2$ (***trans-5***). Under an argon atmosphere, $NaBH_4$ (308 mg, 8.14 mmol) and $^{(iPr)4}$(POCOP)Ir(CO)(H)(Cl) (**6**) (96.3 mg, 0.161 mmol) were added to a 100 mL flask sealed with a Teflon stopcock. To the mixture was added degassed CH_3CN (20 mL) followed by degassed ethanol (15 mL). The resulting yellow solution was stirred overnight at room temperature and turned colorless. Solvent was removed under vacuum giving a white residue. The product was extracted with C_6H_6 (10 mL) and filtered through a pad of diatomaceous earth. Upon lyophilization, ***trans*-5** was isolated as an air-stable white powder; yield: 68 mg (0.12 mmol, 75%). No further purification was necessary. Crystals suitable for diffraction were grown by slow evaporation of a dichloromethane solution. Anal. Calcd. for $C_{19}H_{33}IrO_3P_2$: C, 40.49; H, 5.90. Found: C, 40.07; H, 6.03. ^{1}H NMR (C_6D_6, 300.10 MHz, 25 °C): δ 6.80 (t, $^3J_{HH}$ = 7.7 Hz, 1H; Ar-*H*), 6.68 (d, $^3J_{HH}$ = 7.7 Hz, 2H; Ar-*H*), 1.95 (m, 4H; P-C*H*$(CH_3)_2$), 1.15-0.98 (m, 24H; P-CH(C*H*$_3)_2$), -10.02 (t, $^2J_{PH}$ = 16.5 Hz, 2H; Ir-*H*). ^{31}P{^{1}H} NMR (C_6D_6, 121.49 MHz, 25 °C): δ 173.2 (s). ^{13}C{^{1}H} NMR (C_6D_6, 125.67 MHz, 25 °C): δ 177.42 (m; Ir-*C*O), 163.62 (m; C_{Ar}), 125.33 (s; C_{Ar}), 121.34 (m; C_{Ar}), 104.91 (m; C_{Ar}), 32.55 (vt, $^1J_{PC}$ + $^3J_{PC}$ = 36.7 Hz; P-*C*H$(CH_3)_2$), 17.88 (s; P-CH(*C*H$_3)_2$), 17.36 (s; P-CH(*C*H$_3)_2$). IR (solution, CH_2Cl_2, cm^{-1}): *ν*(CO) 2008, *ν*(H-Ir-H) 1757. IR (solution, C_6D_6, cm^{-1}): *ν*(CO) 2003, *ν*(H-Ir-H) 1762.

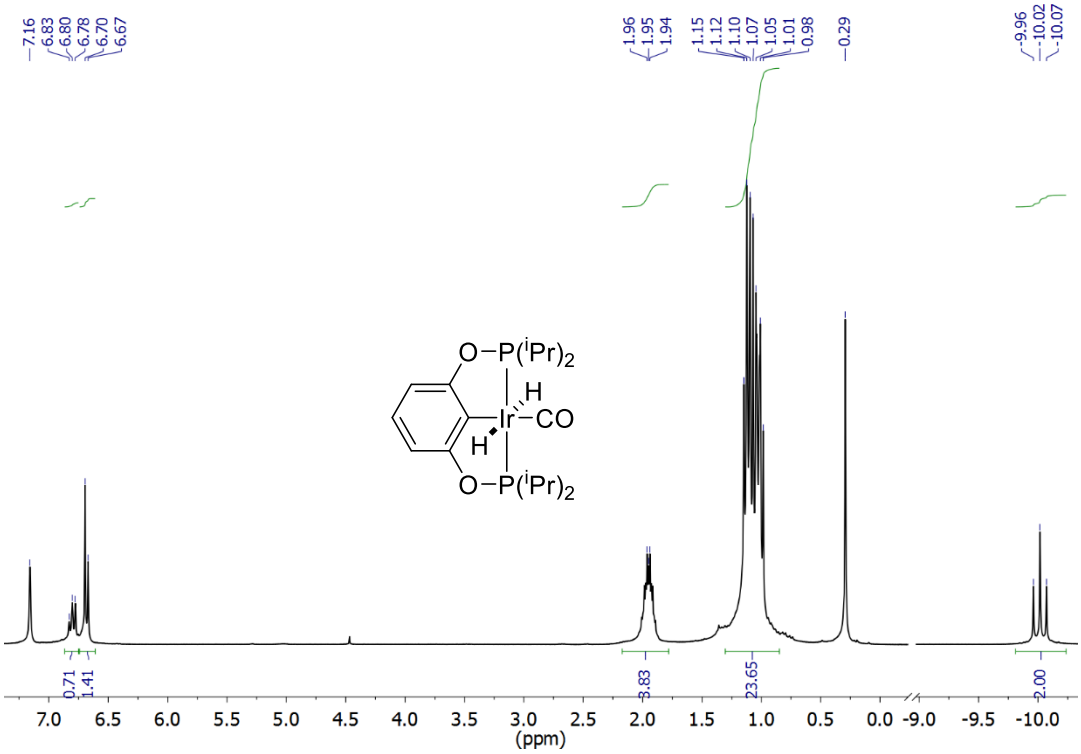

Figure S3. ^{1}H NMR spectrum of *trans-*$^{(iPr)4}$(POCOP)Ir(CO)(H)$_2$ (***trans*-5**) in C_6D_6.

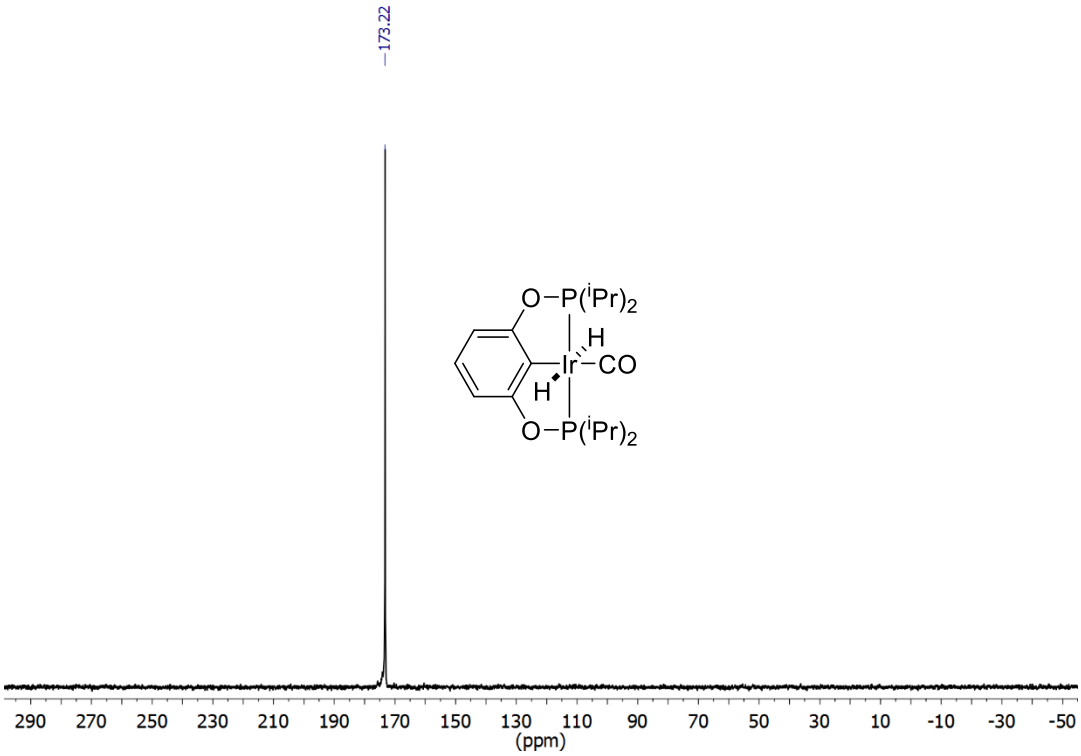

Figure S4. $^{31}P\{^{1}H\}$ NMR spectrum of *trans*-$^{(iPr)4}$(POCOP)Ir(CO)(H)$_2$ (***trans*-5**) in C_6D_6.

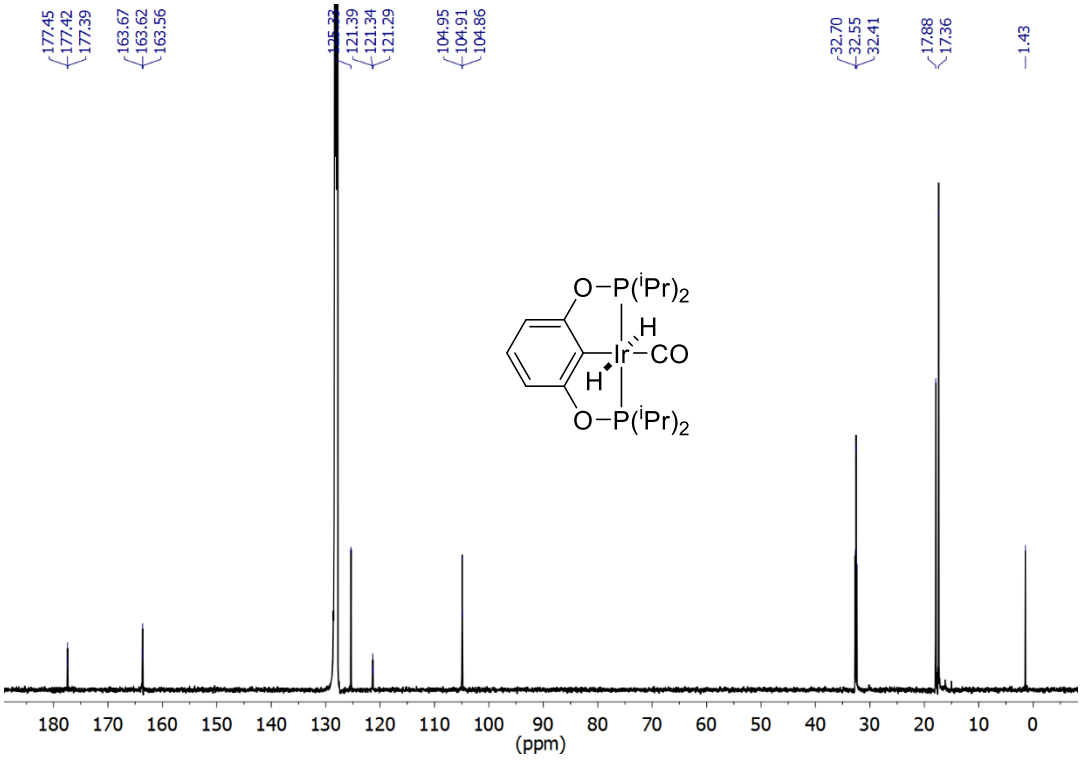

Figure S5. $^{13}C\{^{1}H\}$ NMR spectrum of *trans*-$^{(iPr)4}$(POCOP)Ir(CO)(H)$_2$ (***trans*-5**) in C_6D_6.

Formation of cis-$^{(iPr)4}$*(POCOP)Ir(CO)(H)*$_2$ (***cis*-5**). In a nitrogen-filled glovebox, $^{(iPr)4}$(POCOP)Ir(CO) (**4**) (10 mg, 0.018 mmol) was dissolved in freshly distilled C_6D_6 (0.1 mL) giving a dark yellow solution and was added to a 5 mm thick-walled NMR tube fitted with a Teflon valve. The tube was freeze-pump-thawed three times. The reaction was pressurized with 8 atm H_2 and rotated for 20 min to ensure complete mixing, resulting in a lighter yellow solution. By ^{31}P NMR spectroscopy, 90% conversion to ***cis*-5** was observed. After rotating for 16 h at room temperature, no change in the conversion to ***cis*-5** was observed by ^{31}P NMR spectroscopy. ^{1}H NMR (C_6D_6, 300.13 MHz, 22 °C): δ 6.95-6.80 (m, 3H; Ar-*H*), 2.22 (m, 2H; P-C*H*$(CH_3)_2$), 1.92 (m, 2H; P-C*H*$(CH_3)_2$), 1.18-1.06 (m, 12H; P-CH(C*H*$_3)_2$), 1.01-0.92 (m, 12H; P-CH(C*H*$_3)_2$), -10.30 (t, $^2J_{PH}$ = 9.3 Hz, 1H; Ir-*H*), -11.16 (t, $^2J_{PH}$ = 18.4 Hz, 1H; Ir-*H*). ^{31}P{^{1}H} NMR (C_6D_6, 121.51 Hz, 22 °C): δ 167.7 (s).

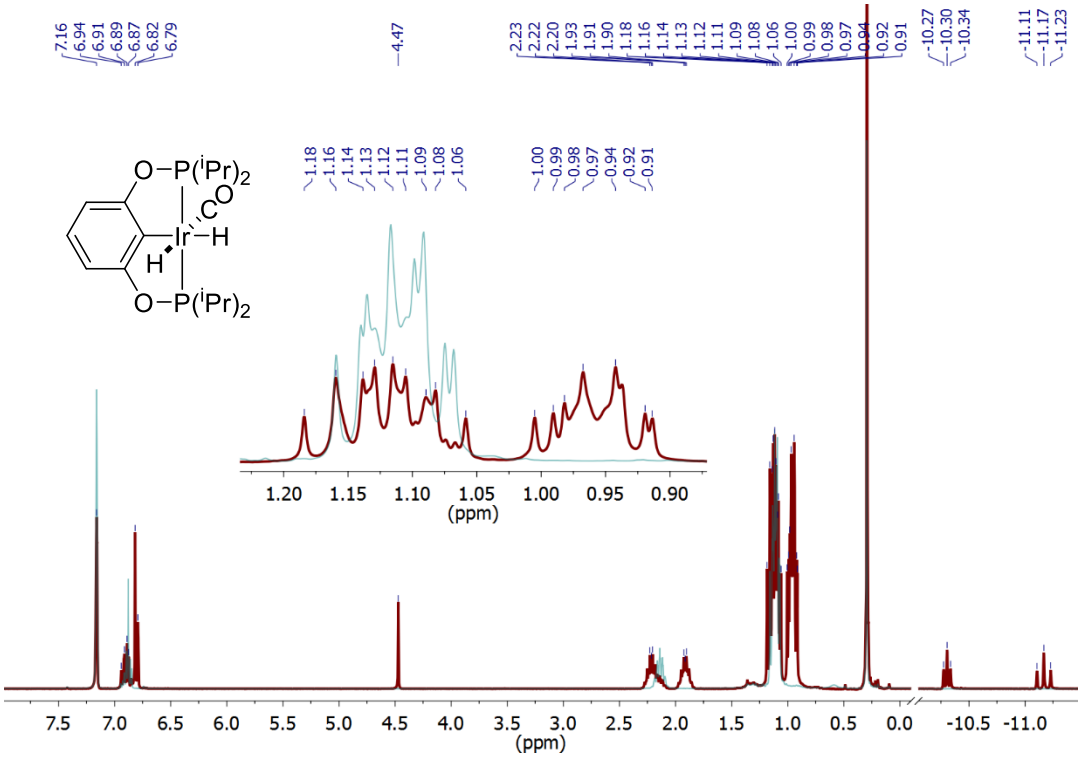

Figure S6. ^{1}H NMR spectrum of *cis*-$^{(iPr)4}$(POCOP)Ir(CO)(H)$_2$ (***cis*-5**) in C_6D_6. Note thicker line shows the *cis*-dihydride complex and the thinner overlay shows $^{(iPr)4}$(POCOP)Ir(CO) (**4**) reference spectrum.

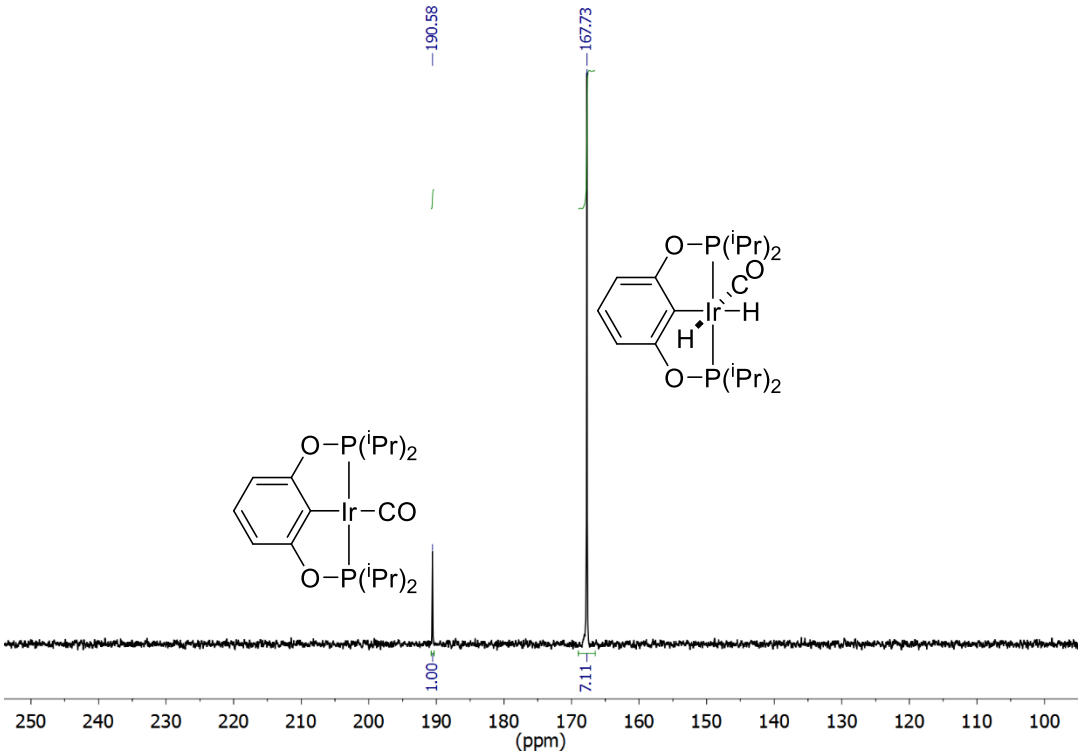

Figure S7. $^{31}P\{^{1}H\}$ NMR spectrum of *cis*-$^{(iPr)4}$(POCOP)Ir(CO)$(H)_2$ (***cis*-5**) in C_6D_6. Note residual $^{(iPr)4}$(POCOP)Ir(CO) (**4**) is observed at 190.6 ppm.

*Synthesis of [$^{(iPr)4}$(POCOP)Ir(CO)(H)(pyr)]BF_4 (**7-BF$_4$**).* In a nitrogen filled glovebox, [Hpyr]BF_4 (24.6 mg, 0.147 mmol) was added to a 20 mL vial containing $^{(iPr)4}$(POCOP)Ir(CO) (**4**) (85 mg, 0.15 mmol). THF (5 mL) and CH_2Cl_2 (2 mL) were added giving a golden yellow solution with undissolved [Hpyr]BF_4. Upon sitting at room temperature for 5 days, the solution color faded to pale yellow and all [Hpyr]BF_4 dissolved. The solution was filtered through a pad of diatomaceous earth and the solvent was removed under vacuum. The yellow/white residue was triturated with pentane then washed with C_6H_6 (3 mL) to remove trace $^{(iPr)4}$(POCOP)Ir(CO) (**4**). The white solid was dried under vacuum then dissolved in CH_2Cl_2 (1 mL) and filtered through diatomaceous earth. Pentane (7 mL) was layered over the CH_2Cl_2 solution and the sample was stored at -30 °C for 5 days giving large colorless plate crystals suitable for diffraction; yield: 68 mg (0.093 mmol, 63%). Anal. Calcd. for $C_{24}H_{37}BF_4IrNO_3P_2$: C, 39.57; H, 5.12; N, 1.92. Found: C, 39.74; H, 5.12; N, 2.01. ^{1}H NMR (CD_2Cl_2, 300.10 MHz, 13 °C): δ 8.90 (br s; C_5H_5N), 8.04 (t, $^{3}J_{HH}$ = 7.6 Hz, 1H; *para*-C_5H_5N), 7.46 (br s; C_5H_5N), 7.18 (t, $^{3}J_{HH}$ = 8.0 Hz, 1H; Ar-*H*), 6.76 (d, $^{3}J_{HH}$ = 8.0 Hz, 2H; Ar-*H*), 2.58 (m, 2H; P-C*H*$(CH_3)_2$), 1.95 (m, 2H; P-C*H*$(CH_3)_2$), 1.24-1.14 (m, 12H; P-CH(C*H*$_3)_2$), 1.06-0.93 (m, 12H; P-CH(C*H*$_3)_2$), -19.46 (t, $^{2}J_{PH}$ = 13.5 Hz, 1H; Ir-*H*). $^{31}P\{^{1}H\}$ NMR (CD_2Cl_2, 121.49 MHz, 13 °C): δ 164.7 (s). $^{13}C\{^{1}H\}$ NMR (CD_2Cl_2, 75.47 MHz, 25 °C): δ 177.53 (m; Ir-*C*O), 164.03 (m; C_{Ar}), 140.93 (s; C_{Ar}), 130.74 (s; C_{Ar}), 128.47 (m; C_{Ar}), 107.49 (m; C_{Ar}), 31.34 (vt, $^{1}J_{PC}$ + $^{3}J_{PC}$ = 33.0 Hz; P-*C*H$(CH_3)_2$), 30.23 (vt, $^{1}J_{PC}$ + $^{3}J_{PC}$ = 36.1 Hz; P-*C*H$(CH_3)_2$), 18.54 (m; P-CH(*C*H$_3)_2$), 17.78 (m; P-CH(*C*H$_3)_2$), 17.61 (m; P-CH(*C*H$_3)_2$), 16.06 (m; P-CH(*C*H$_3)_2$). IR (solution, CH_2Cl_2, cm^{-1}): ν(CO) 2042.

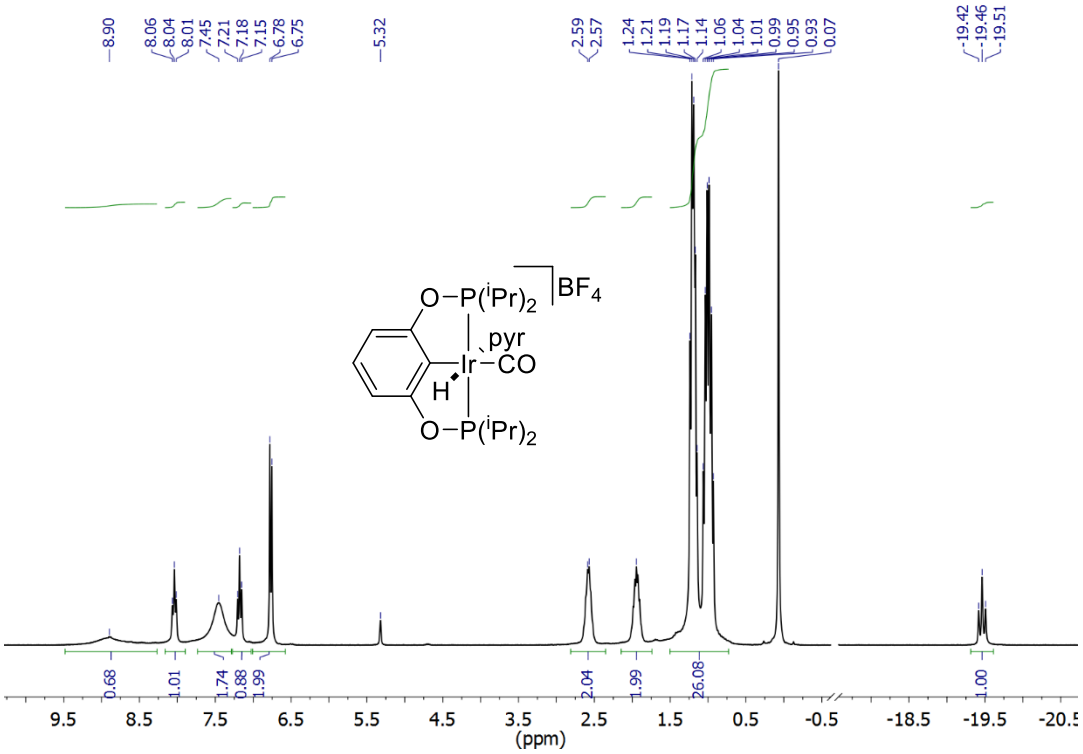

Figure S8. ^{1}H NMR spectrum of [$^{(iPr)4}$(POCOP)Ir(CO)(H)(pyr)]BF_4 (**7-BF$_4$**) in CD_2Cl_2.

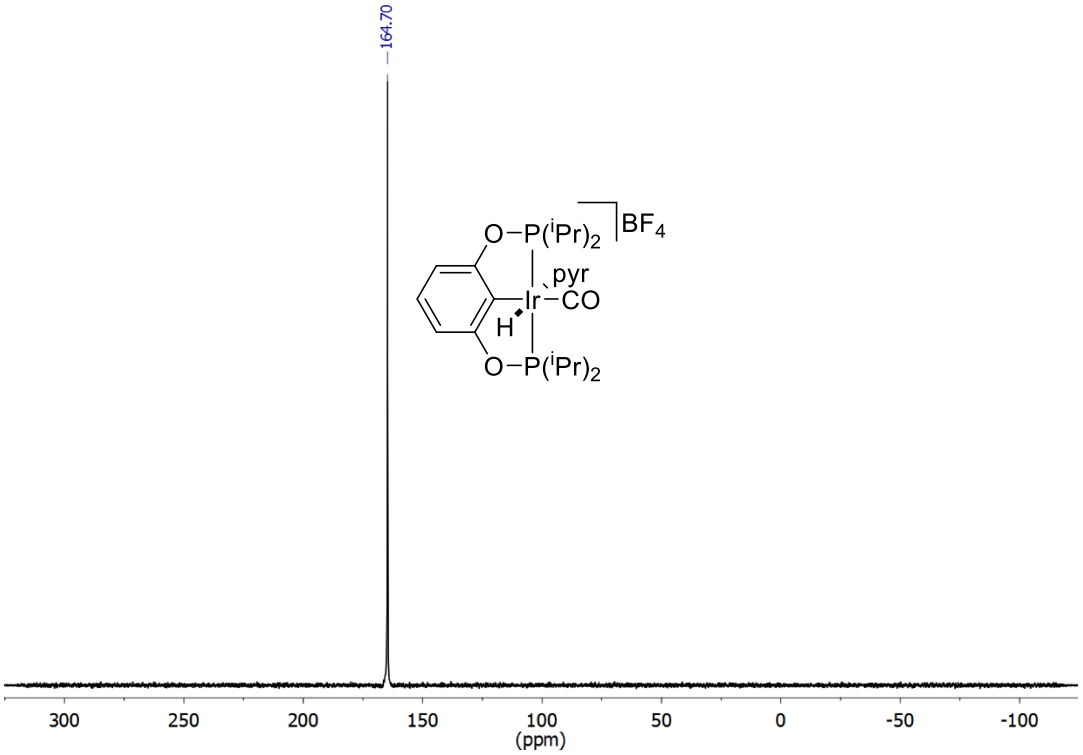

Figure S9. $^{31}P\{^{1}H\}$ NMR spectrum of [$^{(iPr)4}$(POCOP)Ir(CO)(H)(pyr)]BF_4 (**7-BF$_4$**) in CD_2Cl_2.

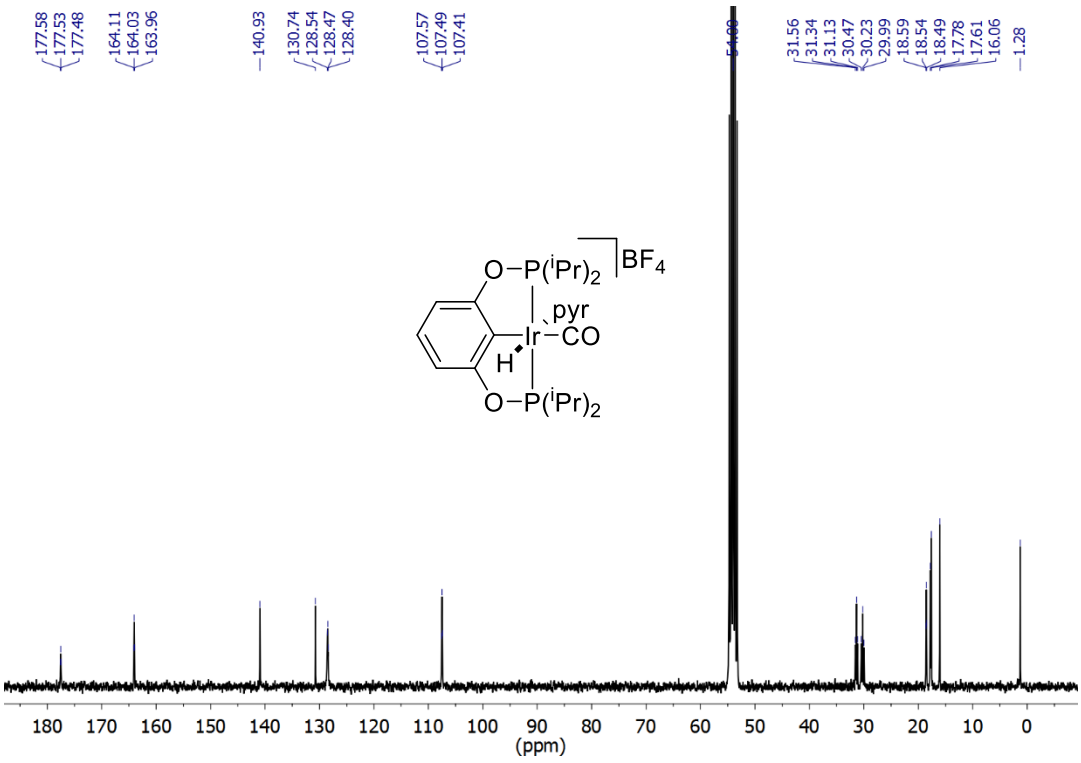

Figure S10. $^{13}C\{^{1}H\}$ NMR (75.47 MHz) spectrum of [$^{(iPr)4}$(POCOP)Ir(CO)(H)(pyr)]BF_4 (**7-BF$_4$**) in CD_2Cl_2.

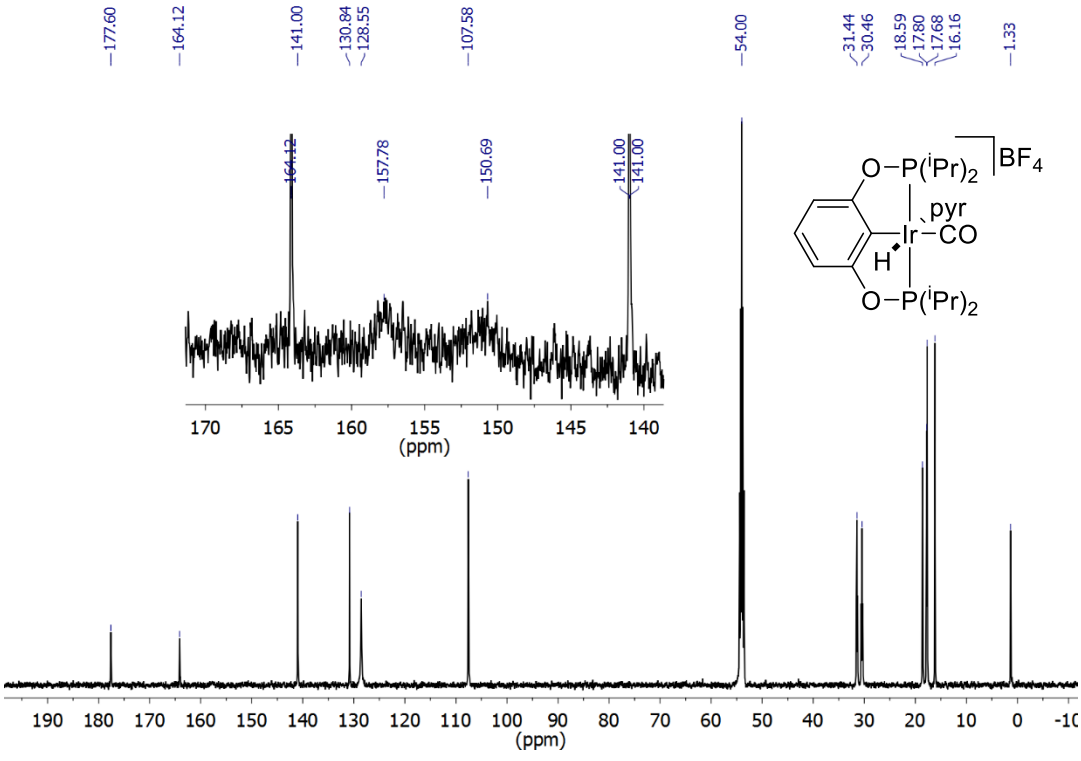

Figure S11. $^{13}C\{^{1}H\}$ NMR (125.77 MHz) spectrum of [$^{(iPr)4}$(POCOP)Ir(CO)(H)(pyr)]BF_4 (**7-BF$_4$**) in CD_2Cl_2. Inset shows broadened resonances assigned to iridium-bound pyridine.

*Preparation of [$^{(tBu)4}$(POCOP)Ir(CO)(H)(pyr)]BArF$_{20}$ (**8**).* An NMR tube fitted with a J. Young style Teflon valve was charged with $^{(tBu)4}$(POCOP)Ir(CO) (**1**) (10 mg, 0.017 mmol), [Hpyr]BArF$_{20}$ (13 mg, 0.017 mmol), and CD_2Cl_2 (0.5 mL) giving a yellow solution. ^{1}H NMR (CD_2Cl_2, 300.13 MHz, 24 °C): δ 8.98 (m, 1H; C_5H_5N), 7.87 (m, 1H; C_5H_5N), 7.46-7.38 (m, 2H; C_5H_5N), 7.25-7.19 (m, 2H; overlapping C_5H_5N and Ar-*H*), 6.84 (m, 2H; Ar-*H*), 1.33 (vt, $^3J_{PH}$ + $^5J_{PH}$ = 15.4 Hz, 18H; P-C(CH_3)$_3$), 1.02 (vt, $^3J_{PH}$ + $^5J_{PH}$ = 15.7 Hz, 18H; P-C(CH_3)$_3$), -19.42 (t, $^2J_{PH}$ = 14.7 Hz, 1H; Ir-*H*). ^{31}P{^{1}H} NMR (CD_2Cl_2, 121.51 MHz, 24 °C): δ 170.0 (s).

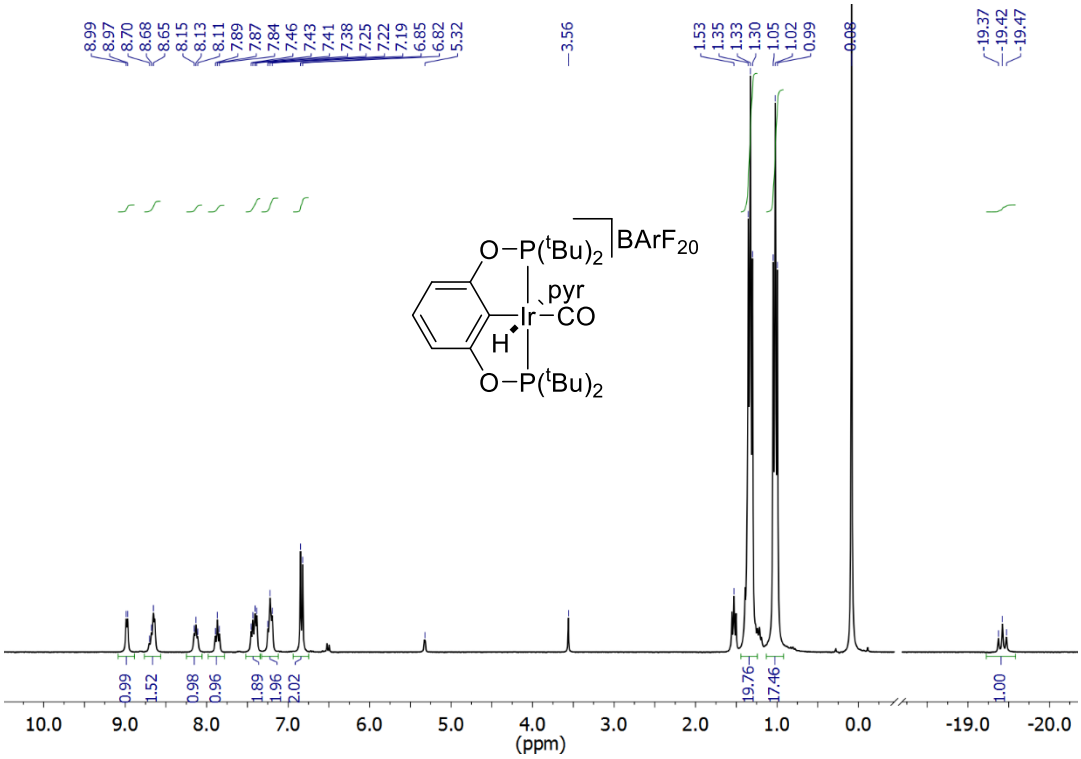

Figure S12. ^{1}H NMR spectrum of [$^{(tBu)4}$(POCOP)Ir(CO)(H)(pyr)]BArF$_{20}$ (**8**) in CD_2Cl_2. Note methanol (3.56 ppm) and *cis*-$^{(tBu)4}$(POCOP)Ir(CO)(H)(Cl) (1.53 ppm) are impurities.

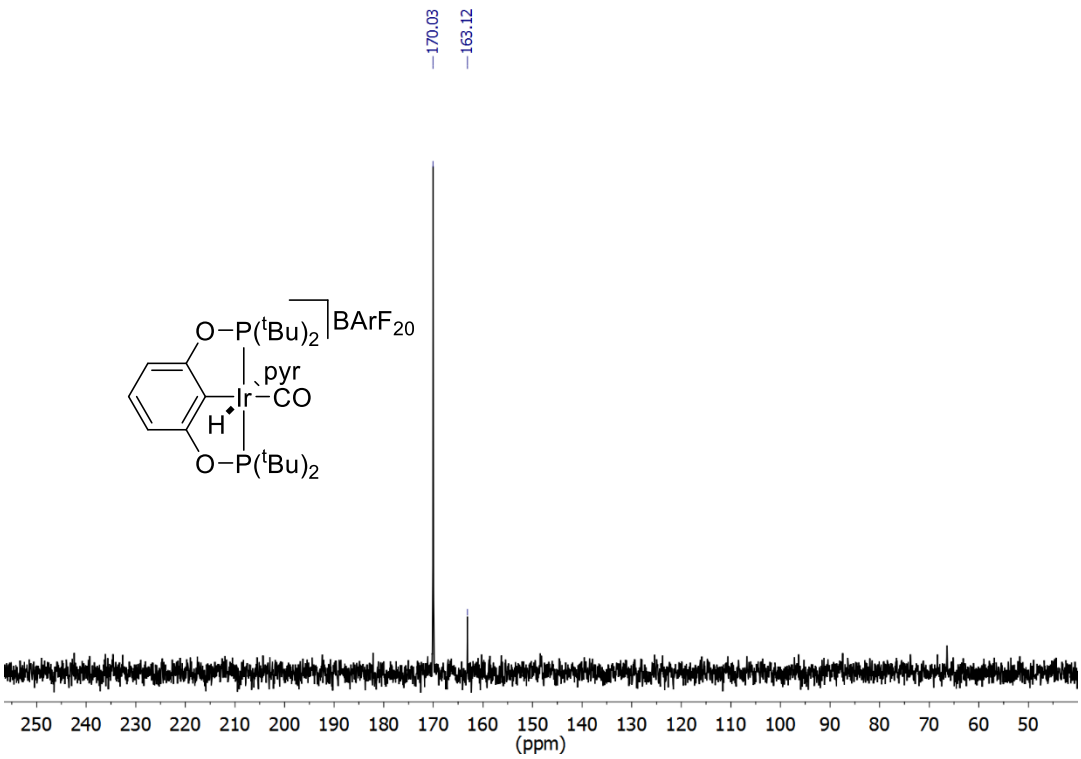

Figure S13. $^{31}P\{^{1}H\}$ NMR spectrum of [$^{(tBu)4}$(POCOP)Ir(CO)(H)(pyr)]$BArF_{20}$ (**8**) in CD_2Cl_2. Note *cis*-$^{(tBu)4}$(POCOP)Ir(CO)(H)(Cl) (163.1 ppm) is an impurity.

*Preparation of $^{(iPr)4}$(POCOP)Ir(CO)(H)(OTs) (**9**).* In an argon filled glovebox, $^{(iPr)4}$(POCOP)Ir(CO) (**4**) (10 mg, 0.018 mmol) and anhydrous *p*-toluenesulfonic acid (16 mg, 0.093 mmol) were added to an NMR tube fitted with a J. Young style Teflon valve. CD_2Cl_2 (0.5 mL) was vacuum transferred into the tube giving a colorless solution. ^{1}H NMR (CD_2Cl_2, 300.10 MHz, 25 °C): δ 7.02 (t, $^{3}J_{HH}$ = 8.1 Hz, 1H; Ar-*H*), 6.62 (d, $^{3}J_{HH}$ = 8.1 Hz, 2H; Ar-*H*), 2.72 (m, 2H; P-C*H*$(CH_3)_2$), 2.53 (m, 2H; P-C*H*$(CH_3)_2$), 1.32-1.23 (m, 12H; P-CH(C*H*$_3)_2$), 1.12 (m, 6H; P-CH(C*H*$_3)_2$), 0.92 (m, 6H; P-CH(C*H*$_3)_2$), -25.17 (t, $^{2}J_{PH}$ = 13.6 Hz, 1H; Ir-*H*). The peaks assignable to bound *p*-toluenesulfonate could not be distinguished from excess *p*TsOH in solution. $^{31}P\{^{1}H\}$ NMR (CD_2Cl_2, 121.49 MHz, 25 °C): δ 170.6 (s).

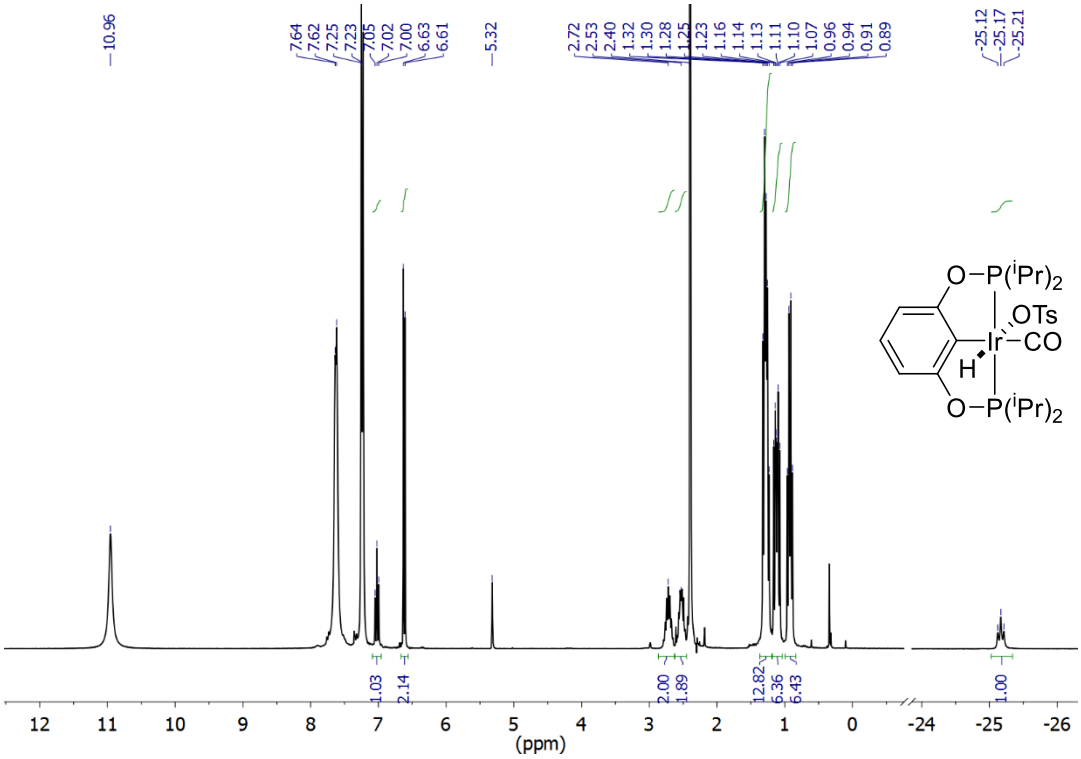

Figure S14. ^{1}H NMR spectrum of $^{(iPr)4}$(POCOP)Ir(CO)(H)(OTs) (**9**) in CD_2Cl_2.

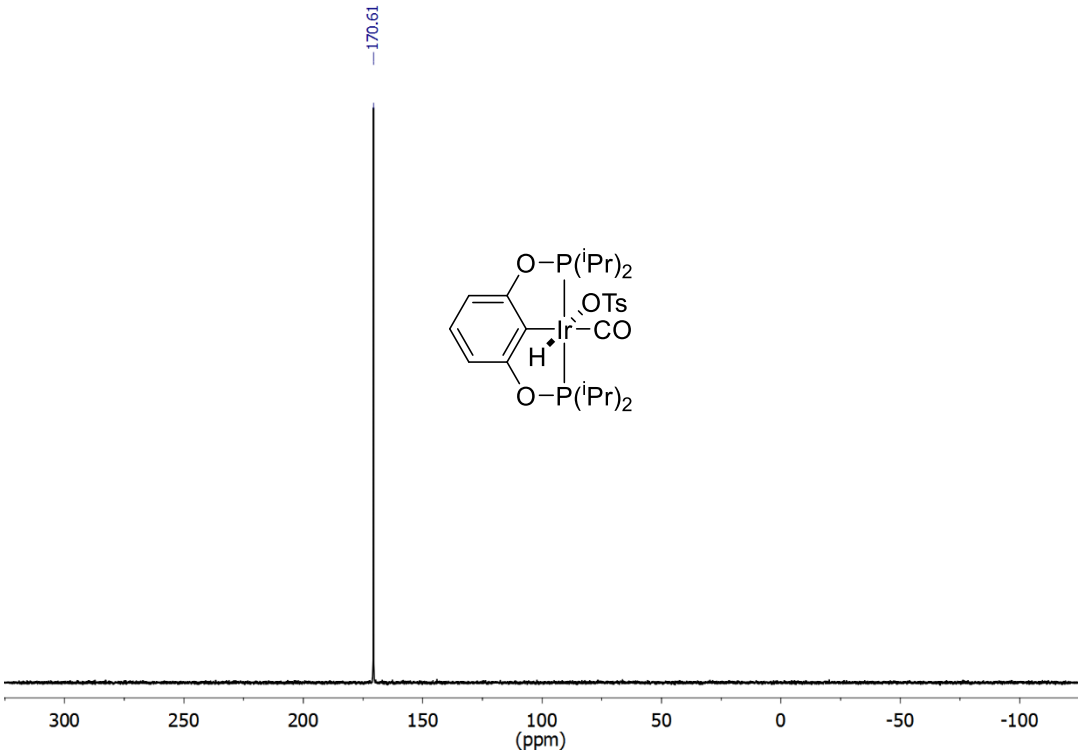

Figure S15. $^{31}P\{^{1}H\}$ NMR spectrum of $^{(iPr)4}$(POCOP)Ir(CO)(H)(OTs) (**9**) in CD_2Cl_2.

*Synthesis of [$^{(tBu)4}$(PCP)Ir(CO)(H)(pyr)]BF_4 (**12**).* $^{(tBu)4}$(PCP)Ir(CO) (**10**) (40 mg, 0.065 mmol) was dissolved in CH_2Cl_2 (10 mL) and [Hpyr]BF_4 (11 mg, 0.065 mmol) added. The solution was left to stand for 15 hours, upon which the solution had turned from yellow to colorless. The solution was filtered through diatomaceous earth and the solvent removed to yield a colorless solid; yield: 46 mg (0.060 mmol, 90%). X-ray diffraction quality crystals were grown from a ternary mixture of CH_2Cl_2, diethyl ether and pentane at -30 °C. ^{1}H NMR (CD_2Cl_2, 499.71 MHz): δ 9.01 (d, $^3J_{HH}$ = 5.9 Hz, 1H; C_5H_5N), 7.88 (t, $^3J_{HH}$ = 7.4 Hz, 1H; C_5H_5N), 7.59 (d, $^3J_{HH}$ = 5.3 Hz, 1H; C_5H_5N), 7.39 (t, $^3J_{HH}$ = 6.1 Hz, 1H; C_5H_5N), 7.29 (d, $^3J_{HH}$ = 7.6 Hz, 2H; Ar-*H*), 7.22 (t, $^3J_{HH}$ = 6.5 Hz, 1H; C_5H_5N), 7.16 (t, $^3J_{HH}$ = 7.4 Hz, 1H; Ar-*H*), 3.57 (dvt, $^2J_{HH}$ = 17.1, $^2J_{PH}$ + $^4J_{PH}$ = 3.9 Hz, 2H; ArCH_2PR_2), 3.39 (dvt, $^2J_{HH}$ = 17.1, $^2J_{PH}$ + $^4J_{PH}$ = 3.6 Hz, 2H; ArCH_2PR_2), 1.26 (vt, $^3J_{PH}$ + $^5J_{PH}$ = 6.9 Hz, 18H; PC(CH_3)$_3$), 1.03 (vt, $^3J_{PH}$ + $^5J_{PH}$ = 6.8 Hz, 18H; PC(CH_3)$_3$), -19.72 (t, $^2J_{PH}$ = 14 Hz, 1H; Ir-*H*). ^{13}C{^{1}H} NMR (CD_2Cl_2, 125.77 MHz): δ 179.59 (m, Ir-*C*O), 160.15 (s; C_{Ar}), 159.93 (m; C_{Ar}), 150.69 (s; C_{Ar}), 149.50 (m; C_{Ar}), 140.02 (s; C_{Ar}), 127.87 (s; C_{Ar}), 127.85 (s; C_{Ar}), 127.41 (s; C_{Ar}), 123.49 (s; C_{Ar}), 38.30 (m; P-*C*(CH_3)$_3$), 37.20 (m; Ar*C*H_2PR_2), 29.80 (m; P-C(*C*H_3)$_3$), 29.57 (m; P-C(*C*H_3)$_3$). ^{31}P NMR (CD_2Cl_2, 202.31 MHz): δ 60.8 (s). Anal. Calcd. for $C_{30}H_{49}BF_4IrNOP_2$: C, 46.15; H, 6.33; N, 1.79. Found: C, 46.15; H, 6.15, N, 1.69. IR (solution, CH_2Cl_2, cm^{-1}): ν(CO) 2018.

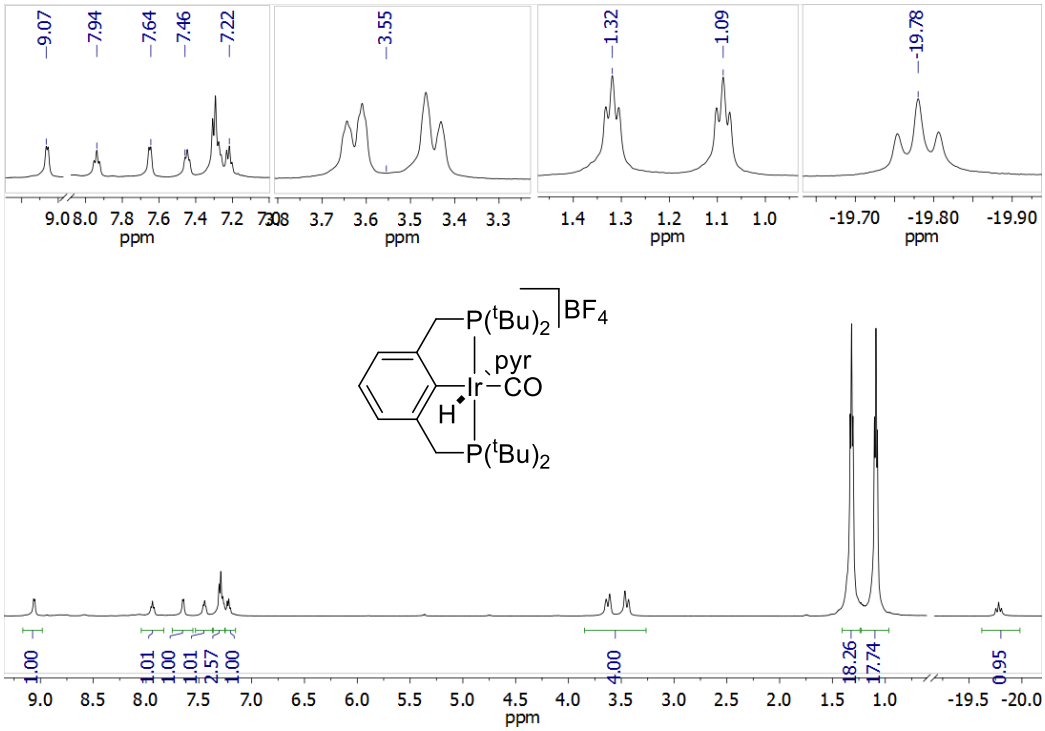

Figure S16. ^{1}H NMR spectrum of [$^{(tBu)4}$(PCP)Ir(CO)(H)(pyr)]BF_4 (**12**) in CD_2Cl_2.

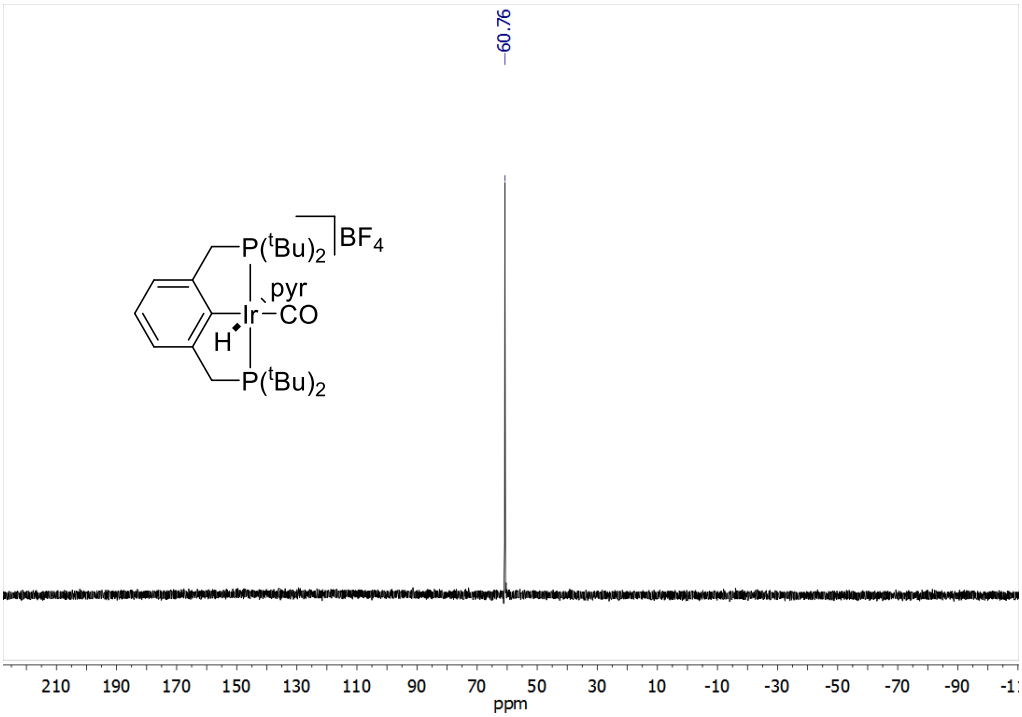

Figure S17. $^{31}P\{^{1}H\}$ NMR spectrum of [$^{(tBu)4}$(PCP)Ir(CO)(H)(pyr)]BF_4 (**12**) in CD_2Cl_2.

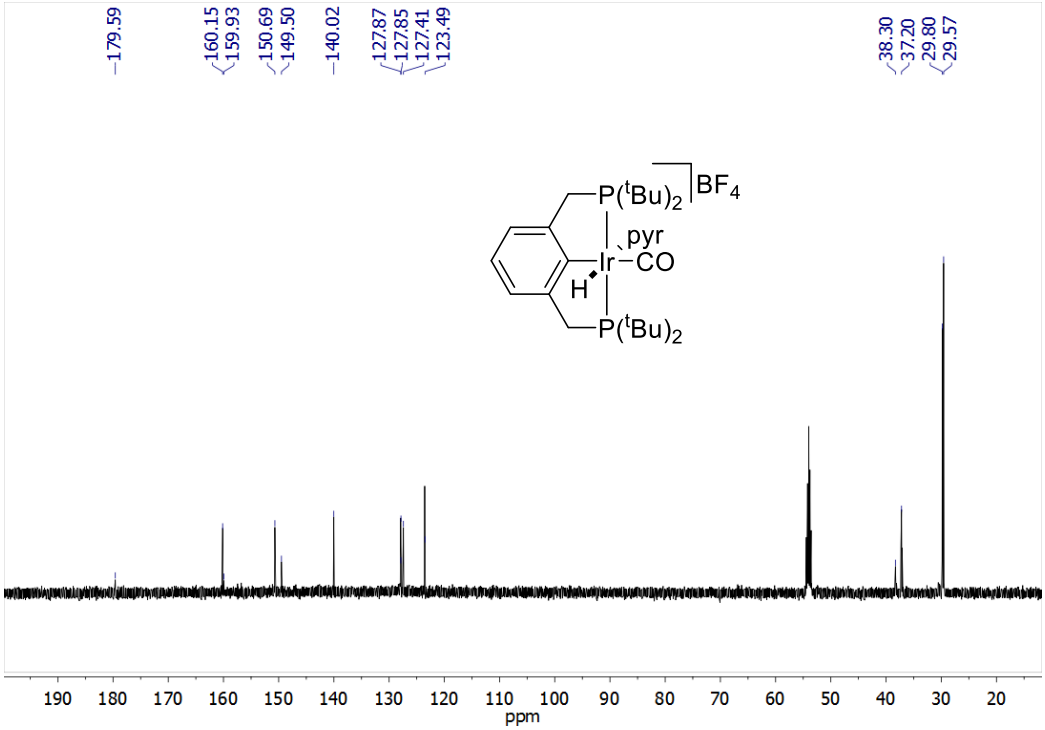

Figure S18. $^{13}C\{^{1}H\}$ NMR spectrum of [$^{(tBu)4}$(PCP)Ir(CO)(H)(pyr)]BF_4 (**12**) in CD_2Cl_2.

Recrystallization of **13** from pentane at -35°C under an N_2 atmosphere led to the crystallization of **[$^{(iPr)4}$(PCP)Ir]$_2$(μ-N$_2$)**.
^{1}H NMR (C_6D_6, 499.71 MHz,) δ 7.20 (d, $^3J_{HH}$ = 7.3 Hz, 2H; Ar-*H*), 7.08 (t, $^3J_{HH}$ = 7.3 Hz, 1H; Ar-*H*), 3.03 (vt, $^2J_{PH}$ + $^4J_{PH}$ = 3.3 Hz, 4H; ArC*H*$_2$PR$_2$), 2.14 (m, 4H; PC*H*(CH$_3$)$_2$), 1.33 (m, 12H; PCH(C*H*$_3$)$_2$), 1.10 (m, 12H; PCH(C*H*$_3$)$_2$). ^{31}P{^{1}H} NMR (C_6D_6, 202.31 MHz): δ 59.5 (s). See X-ray crystallography section for ORTEP.

*Synthesis of [$^{(iPr)4}$(PCP)Ir(CO)(H)(pyr)]BF$_4$ (**15**).* $^{(iPr)4}$(PCP)Ir(CO) (**13**) (98 mg, 0.18 mmol) was dissolved in CH_2Cl_2 (5 mL) and [Hpyr]BF$_4$ (29 mg, 0.18 mmol) added. The solution was left to stand for 48 hours, upon which the solution had turned from orange to yellow. The solution was filtered through diatomaceous earth and the solvent removed to yield a yellow solid which was recrystallized from a ternary mixture of CH_2Cl_2, diethyl ether and pentane at -30 ºC; yield: 115 mg (0.16 mmol, 91 %). ^{1}H NMR (CD_2Cl_2, 300.10 MHz): δ 8.25 (br s, 2H; C$_5$*H*$_5$N), 7.98 (t, $^3J_{HH}$ = 8.0 Hz, 1H; Ar-*H*), 7.39 (t, $^3J_{HH}$ = 6.9 Hz, 2H; C$_5$*H*$_5$N), 7.19 (m, 3H, Ar-*H*), 3.58 (dvt, $^2J_{HH}$= 17.7, $^2J_{PH}$ + $^4J_{PH}$ = 4.6 Hz, 2H; ArC*H*$_2$PR$_2$), 3.34 (dvt, $^2J_{HH}$ = 17.7, $^2J_{PH}$ + $^4J_{PH}$ = 4.1 Hz, 2H; ArC*H*$_2$PR$_2$), 2.34 (m, 2H; PC*H*(CH$_3$)$_2$), 1.90 (m, 2H; PC*H*(CH$_3$)$_2$), 1.07 (m, 24H; PCH(C*H*$_3$)$_2$), -19.15 (t, $^2J_{PH}$ = 12 Hz, 1H; Ir-*H*). ^{31}P{^{1}H} NMR (CD_2Cl_2, 121.49 MHz): δ 47.8 (s). IR (solution, CH_2Cl_2, cm^{-1}): ν(CO) 2023.

Experimental procedures

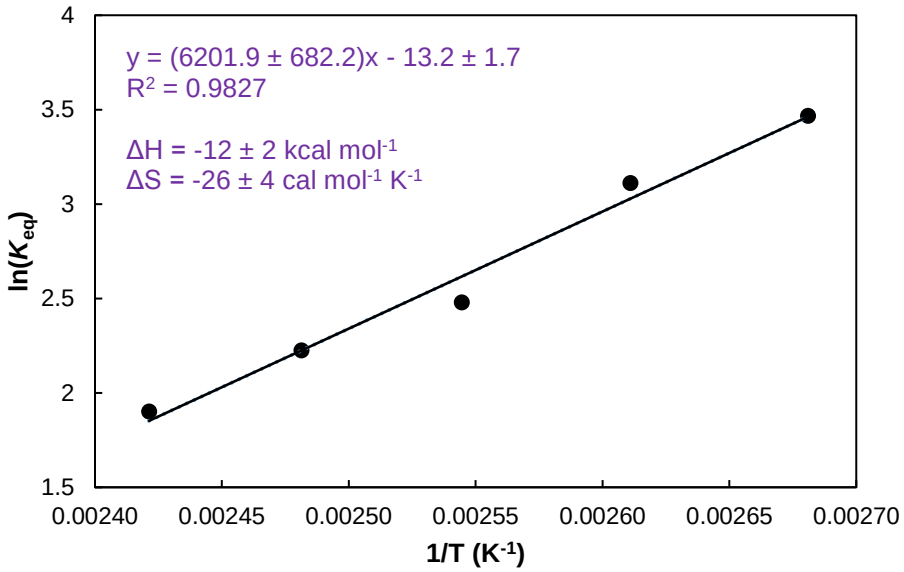

Figure S19. van't Hoff plot for equilibrium between ***cis*-5** and ***trans*-5** in mesitylene.

*Low temperature CO addition to $^{(tBu)4}$(POCOP)Ir(H)$_2$ (**16**).* In an argon-filled glovebox, $^{(tBu)4}$(POCOP)Ir(H)$_2$ (**16**) (8.5 mg, 0.014 mmol) was added to an NMR tube fitted with a J. Young style Teflon valve. Toluene-d_8 (~0.5 mL) was vacuum transferred into the tube, resulting in a red

solution. The sample was freeze-pump-thawed three times. The tube was cooled to -78 °C and pressurized with 1 atm CO followed by immediate cooling to -196 °C. The sample was thawed to -78 °C and immediately inserted into a pre-cooled NMR probe at -63 °C.

*Isomerization of cis- to trans-$^{(iPr)4}$(POCOP)Ir(CO)(H)$_2$ (**cis-5** to **trans-5**).* Heating the sample containing ~90% ***cis*-5** for 88 h at 100 °C under 8 atm H_2 in a 5 mm thick-walled NMR tube fitted with a Teflon valve results in 95% conversion to ***trans*-5** by ^{31}P NMR spectroscopy. The remaining 5% is ***cis*-5**.

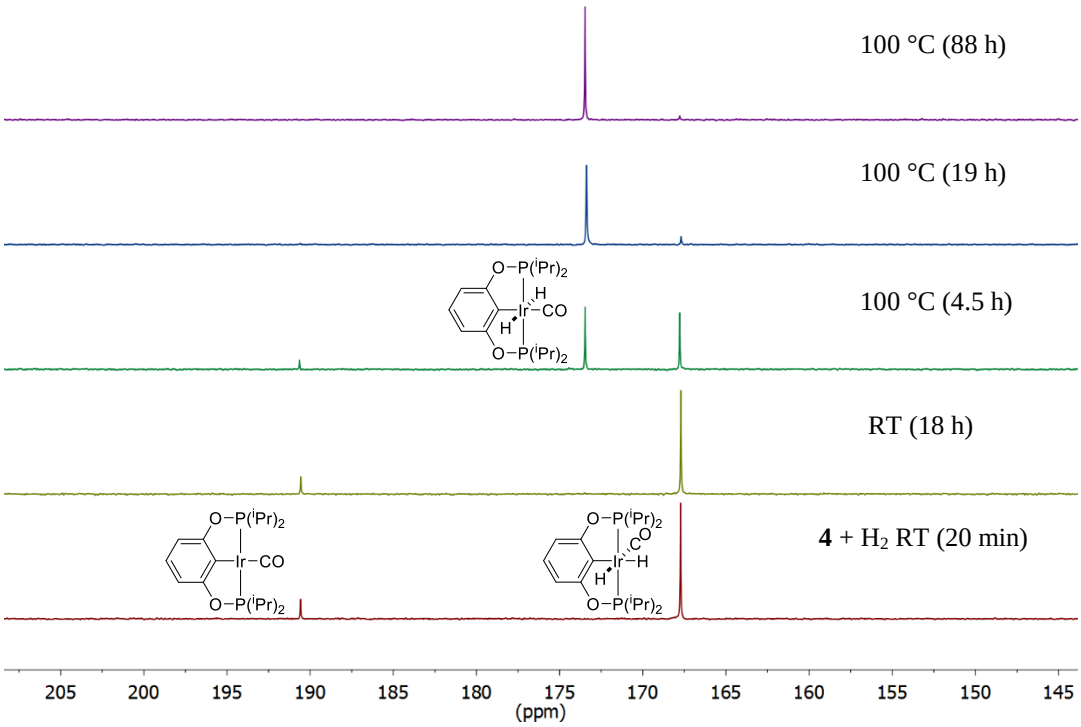

Figure S20. Stacked ^{31}P{^{1}H} NMR spectra of *cis*- to *trans*-$^{(iPr)4}$(POCOP)Ir(CO)(H)$_2$ (***cis*-5** to ***trans*-5**) isomerization.

*Reaction of $^{(tBu)4}$(POCOP)Ir(CO) (**1**) with H_2 (acid catalyzed with [Hpyr]BF_4).* In a nitrogen-filled glovebox, [Hpyr]BF_4 (4 μL, 1.0 M in CH_3CN, 0.004 mmol) was added to a 5 mm thick-walled NMR tube fitted with a Teflon valve. Solvent was removed under vacuum. A solution of $^{(tBu)4}$(POCOP)Ir(CO) (**1**) (4 mg, 0.007 mmol) in THF-d_8 was added to the tube; some undissolved [Hpyr]BF_4 and **1** was observed. The sample was freeze-pump-thawed three times and pressurized with 8 atm H_2.

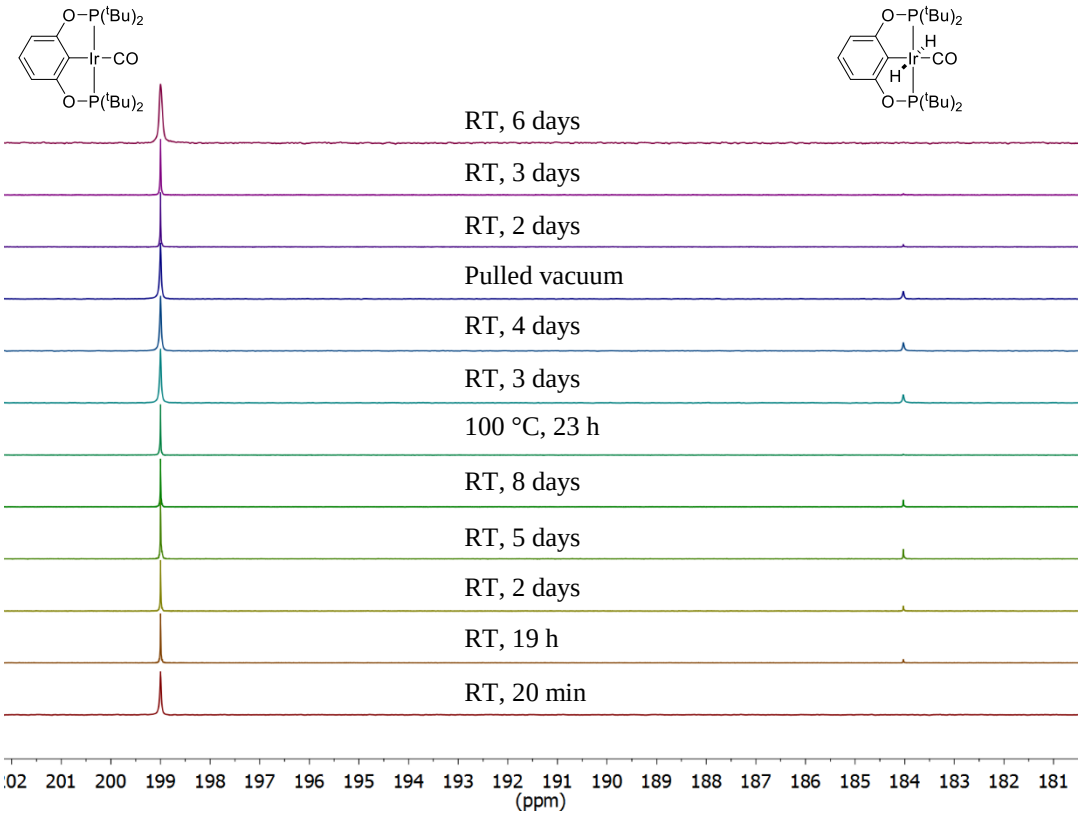

Figure S21. Stacked $^{31}P\{^{1}H\}$ NMR spectra of proton-catalyzed hydrogen addition to $^{(tBu)4}$(POCOP)Ir(CO) (**1**) with [Hpyr]BF_4 in THF-d_8.

*Reaction of $^{(tBu)4}$(POCOP)Ir(CO) (**1**) and [$^{(tBu)4}$(POCOP)Ir(CO)(H)]BF_4 (**3-BF_4**) with H_2.* In a nitrogen-filled glovebox, [$^{(tBu)4}$(POCOP)Ir(CO)(H)]BF_4 (**3-BF_4**) (4 mg, 0.006 mmol) and $^{(tBu)4}$(POCOP)Ir(CO) (**1**) (5.6 mg, 0.0091 mmol) were dissolved in CD_2Cl_2, giving a yellow solution and transferred to a 5 mm thick-walled NMR tube fitted with a Teflon valve. The sample was freeze-pump-thawed three times and pressurized with 8 atm H_2.

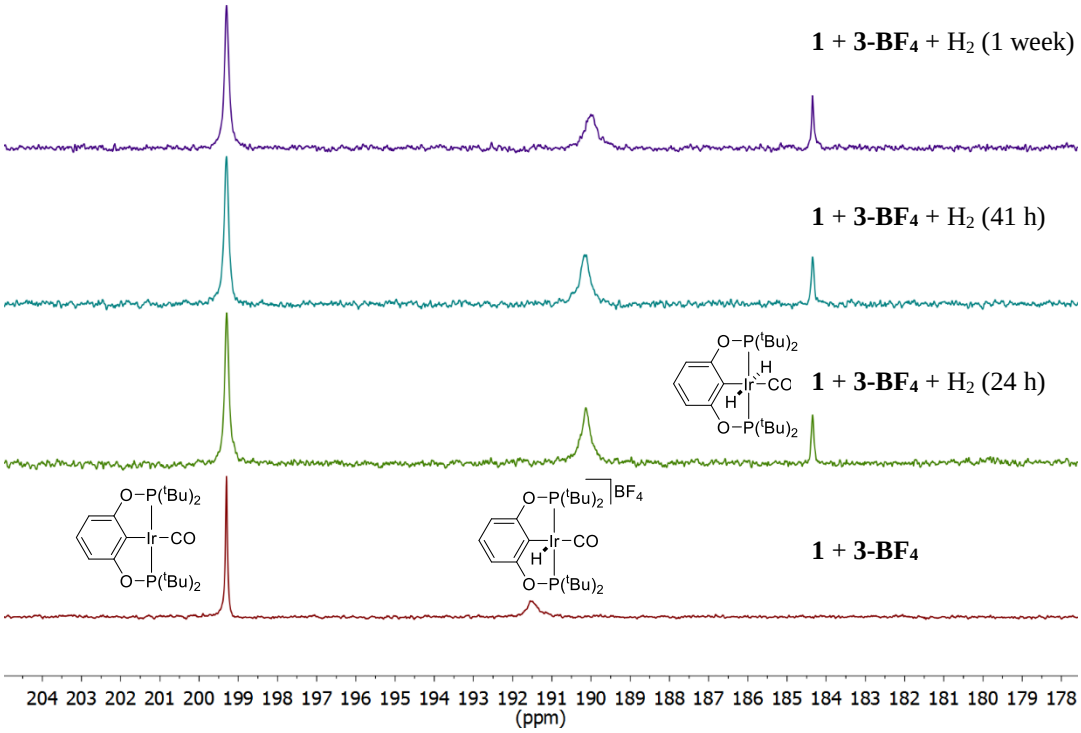

Figure S22. Stacked $^{31}P\{^{1}H\}$ NMR spectra of proton-catalyzed hydrogen addition to $^{(tBu)4}$(POCOP)Ir(CO) (**1**) with [$^{(tBu)4}$(POCOP)Ir(CO)(H)]BF_4 (**3-BF$_4$**) in CD_2Cl_2.

*Reaction of $^{(iPr)4}$(POCOP)Ir(CO) (**4**) with H_2 (acid catalyzed with [Hlut]BF_4).* In a nitrogen-filled glovebox, [Hlut]BF_4 (20 μL, 505 mM in CH_3CN, 0.010 mmol) was added to a 5 mm thick-walled NMR tube fitted with a Teflon valve. Solvent was removed under vacuum. A solution of $^{(iPr)4}$(POCOP)Ir(CO) (**4**) (11 mg, 0.020 mmol) in THF-d_8 was added to the tube giving a dark yellow solution. The sample was freeze-pump-thawed three times and pressurized with 8 atm H_2. After mixing for 2 days, the solution turned colorless.

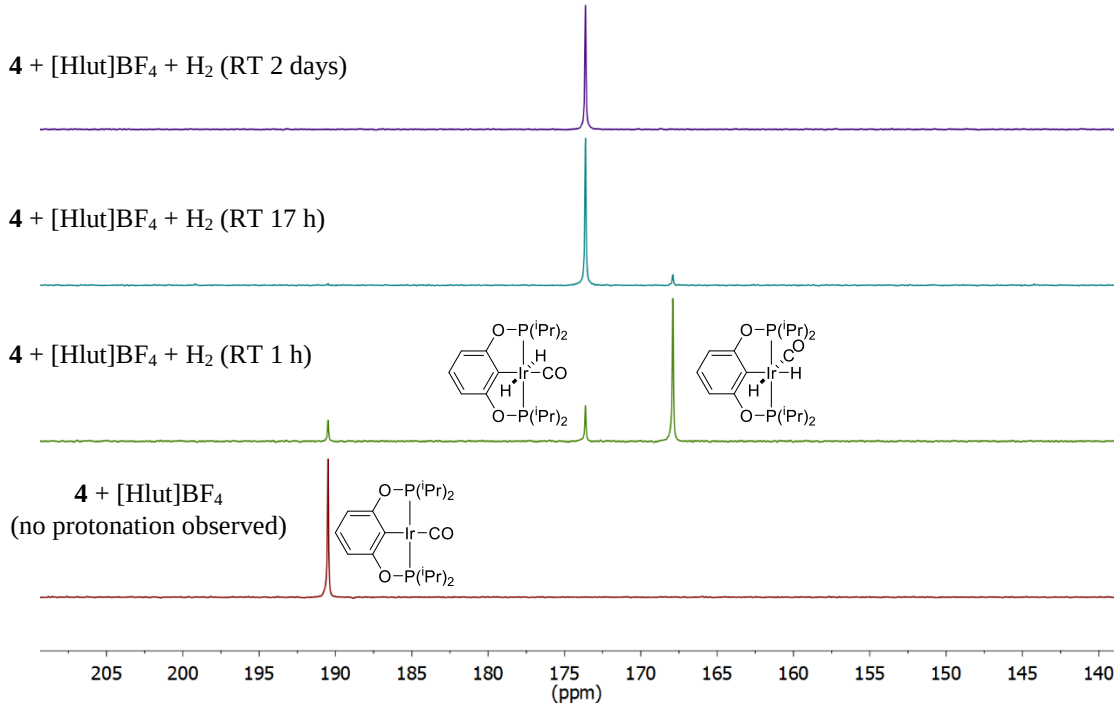

Figure S23. Stacked $^{31}P\{^{1}H\}$ NMR spectra of proton-catalyzed hydrogen addition to $^{(iPr)4}$(POCOP)Ir(CO) (**4**) with [Hlut]BF_4 in THF-d_8.

*Reaction of $^{(iPr)4}$(POCOP)Ir(CO) (**4**) with H_2 (acid catalyzed with [Hpyr]BF_4).* In a nitrogen-filled glovebox, [Hpyr]BF_4 (8 μL, 1 M in CH_3CN, 0.008 mmol) was added to a 5 mm thick-walled NMR tube fitted with a Teflon valve. Solvent was removed under vacuum. A solution of $^{(iPr)4}$(POCOP)Ir(CO) (**4**) (10 mg, 0.018 mmol) in THF-d_8 was added to the tube; some undissolved [Hpyr]BF_4 was observed. The sample was freeze-pump-thawed three times and pressurized with 8 atm H_2.

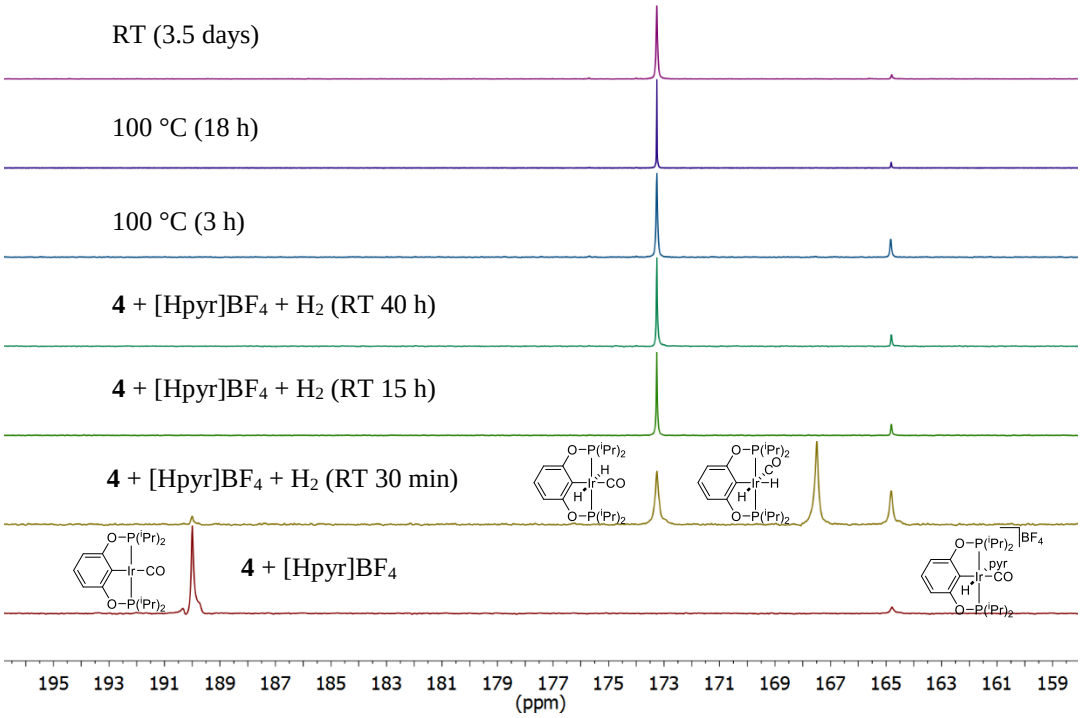

Figure S24. Stacked $^{31}P\{^{1}H\}$ NMR spectra of proton-catalyzed hydrogen addition to $^{(iPr)4}$(POCOP)Ir(CO) (**4**) with [Hpyr]BF_4 in THF-d_8.

*Reaction of $^{(iPr)4}$(POCOP)Ir(CO) (**4**) with H_2 (acid catalyzed with [Hpyr]$BArF_{20}$).* In a nitrogen-filled glovebox, [Hpyr]$BArF_{20}$ (97 μL, 100 mM in CH_3CN, 0.0097 mmol) was added to a 5 mm thick-walled NMR tube fitted with a Teflon valve. Solvent was removed under vacuum. A solution of $^{(iPr)4}$(POCOP)Ir(CO) (**4**) (11 mg, 0.020 mmol) in THF-d_8 was added to the tube giving a dark yellow solution. The sample was freeze-pump-thawed three times and pressurized with 8 atm H_2. After mixing for 17 h, the solution turned colorless.

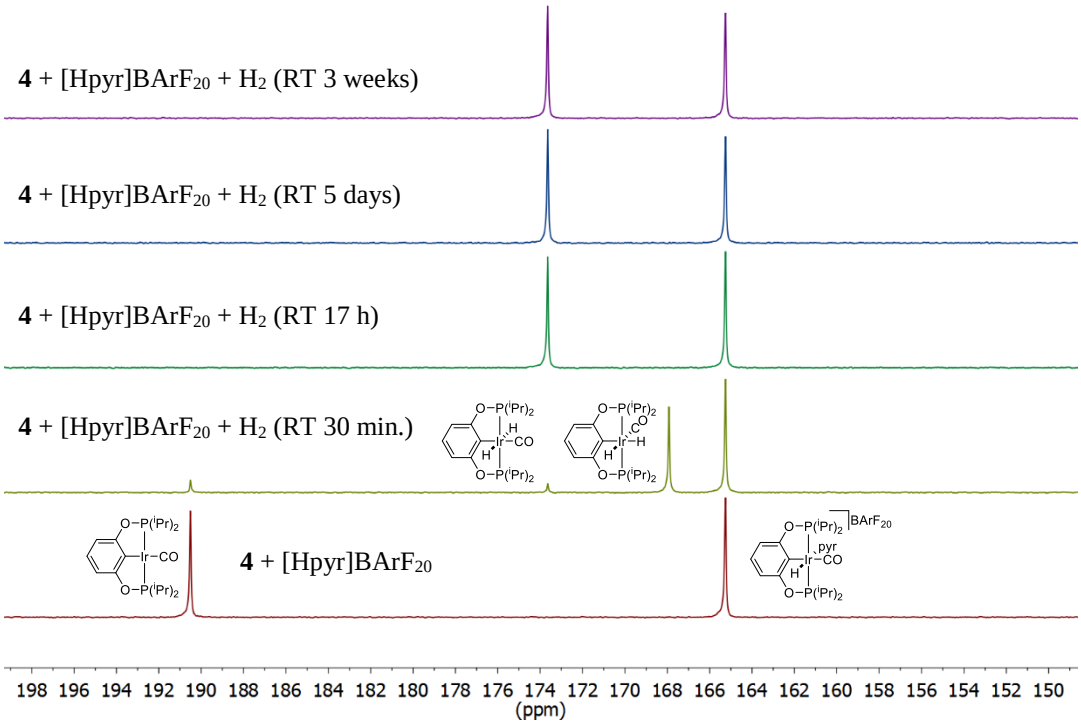

Figure S25. Stacked $^{31}P\{^{1}H\}$ NMR spectra of proton-catalyzed hydrogen addition to $^{(iPr)4}$(POCOP)Ir(CO) (**4**) with [Hpyr]BArF$_{20}$ in THF-d_8.

*Reaction of $^{(iPr)4}$(POCOP)Ir(CO) (**4**) and [$^{(iPr)4}$(POCOP)Ir(CO)(H)(pyr)]BF$_4$ (**7-BF$_4$**) with H$_2$.* In a nitrogen-filled glovebox, [$^{(iPr)4}$(POCOP)Ir(CO)(H)(pyr)]BF$_4$ (**7-BF$_4$**) (5 mg, 0.007 mmol) was dissolved in 50 μL CH_2Cl_2 and added to a 5 mm thick-walled NMR tube fitted with a Teflon valve. The solvent was removed under vacuum. A yellow solution of $^{(iPr)4}$(POCOP)Ir(CO) (**4**) (10.5 mg, 0.0187 mmol) in THF-d_8 was added to the tube; some **7-BF$_4$** was undissolved. The sample was freeze-pump-thawed three times and pressurized with 8 atm H_2. After mixing for 4 days, the solution turned colorless. Minor impurities observed by ^{31}P NMR after 4 days at room temperature are at 148.2 and 139.4 ppm. After pulling vacuum on the sample, the solution turned pale yellow.

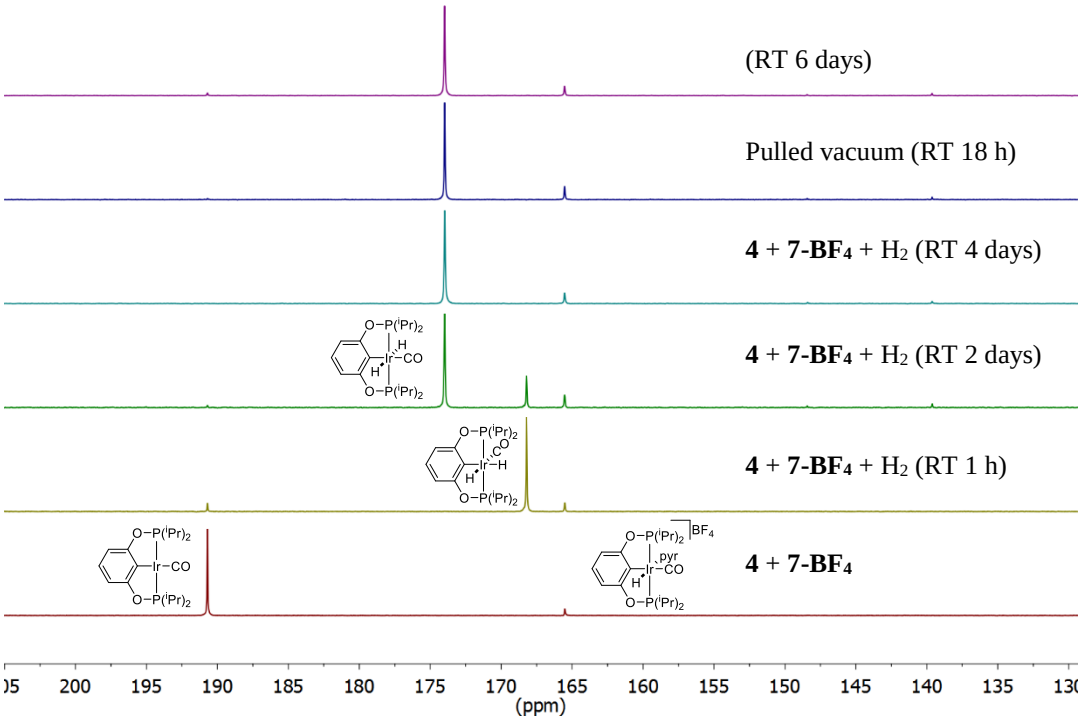

Figure S26. Stacked $^{31}P\{^{1}H\}$ NMR spectra of proton-catalyzed hydrogen addition to $^{(iPr)4}$(POCOP)Ir(CO) (**4**) with [$^{(iPr)4}$(POCOP)Ir(CO)(H)(pyr)]BF_4 (**7-BF$_4$**) in THF-d_8.

*Reaction of trans-$^{(iPr)4}$(POCOP)Ir(CO)(H)$_2$ (**trans-5**) with [Hpyr]BArF$_{20}$.* In air, *trans*-$^{(iPr)4}$(POCOP)Ir(CO)(H)$_2$ (***trans*-5**) (7.1 mg, 0.013 mmol) was added to an NMR tube fitted with a J. Young style Teflon valve and evacuated on a vacuum line. In a nitrogen-filled glovebox, [Hpyr]BArF$_{20}$ (10.4 mg, 0.0137 mmol) was added followed by THF-d_8 giving a colorless solution. After mixing at room temperature for 6 days, full conversion to [$^{(iPr)4}$(POCOP)Ir(CO)(H)(pyr)]BArF$_{20}$ (**7-BArF$_{20}$**) was observed by NMR spectroscopy. No color changes were observed.

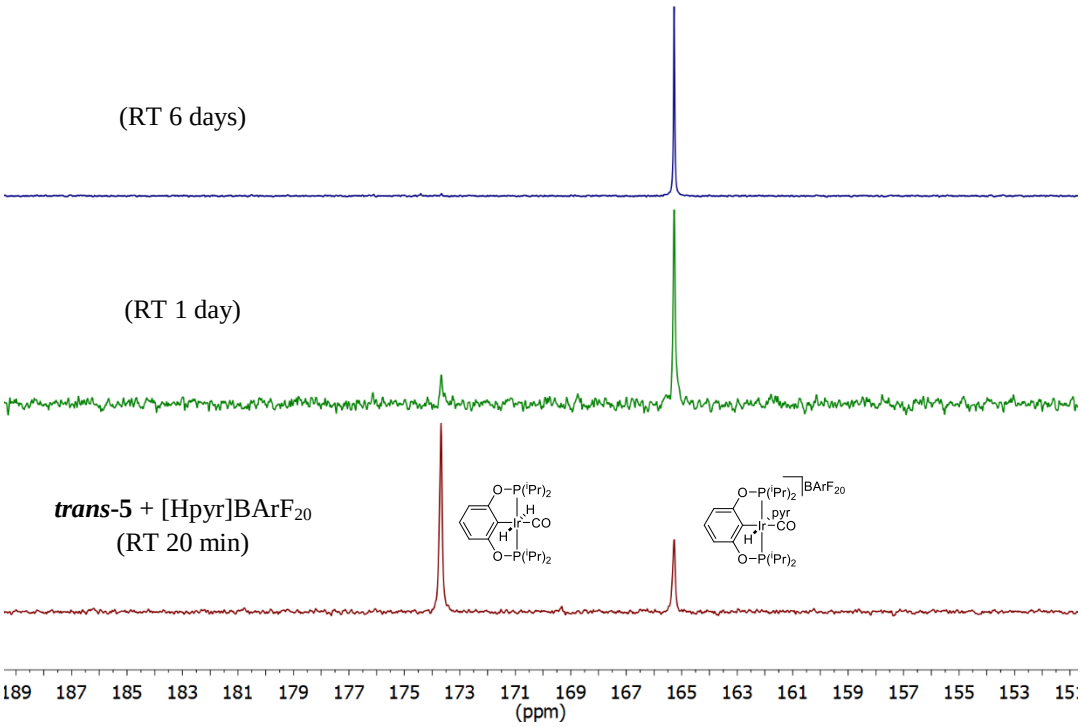

Figure S27. Stacked $^{31}P\{^{1}H\}$ NMR spectra of reaction of *trans*-$^{(iPr)4}$(POCOP)Ir(CO)(H)$_2$ (***trans*-5**) with [Hpyr]BArF$_{20}$ in THF-d_8.

*Low temperature protonation of trans-$^{(iPr)4}$(POCOP)Ir(CO)(H)$_2$ (**trans-5**) with pTsOH.* In air, *trans*-$^{(iPr)4}$(POCOP)Ir(CO)(H)$_2$ (***trans*-5**) (11.0 mg, 0.0195 mmol) was added to an NMR tube fitted with a J. Young style Teflon valve and evacuated on a vacuum line. In a nitrogen-filled glovebox, anhydrous *p*-toluenesulfonic acid (~25 mg, 0.15 mmol) was added to the tube. CD_2Cl_2 was vacuum transferred and the sample was maintained at -196 °C. The sample was thawed to -78 °C and immediately inserted into a pre-cooled NMR probe at -80 °C. Formation of $^{(iPr)4}$(POCOP)Ir(CO)(H)(OTs) (**9**) was immediately observed by NMR spectroscopy.

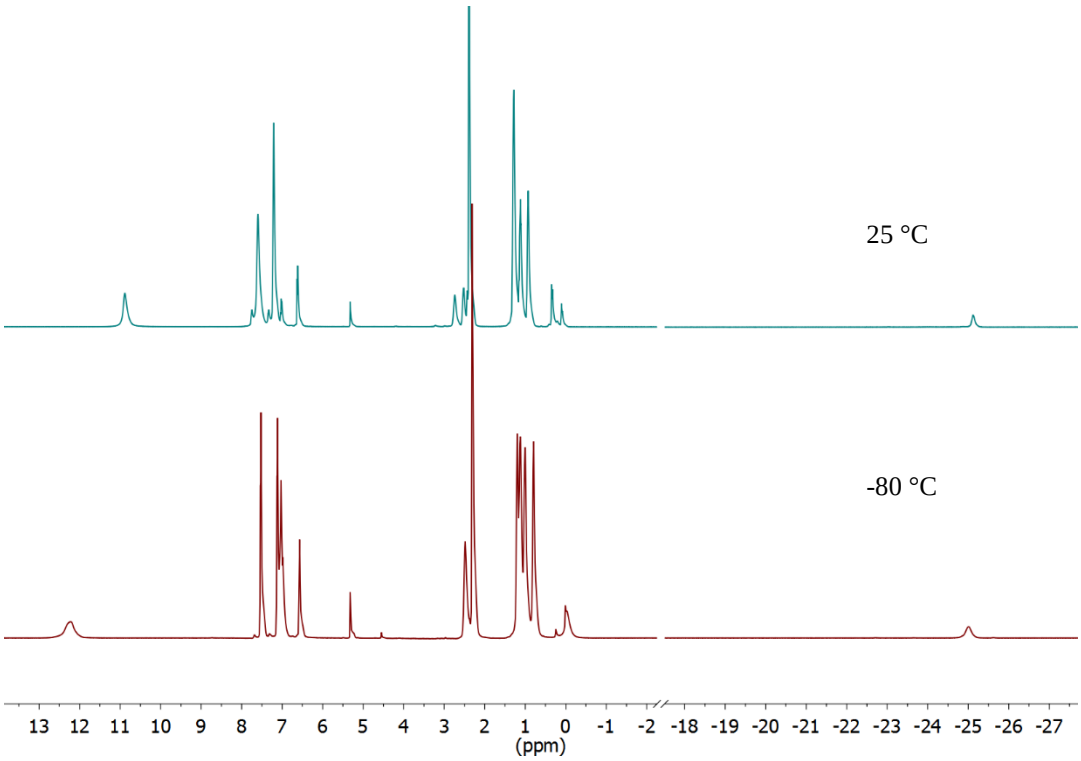

Figure S28. Stacked ^{1}H NMR spectra of low temperature protonation of *trans*-$^{(iPr)4}$(POCOP)Ir(CO)(H)$_2$ (***trans*-5**) with *p*TsOH in CD_2Cl_2.

*Reaction of $^{(tBu)4}$(PCP)Ir(CO) (**10**) with H_2.* $^{(tBu)4}$(PCP)Ir(CO) (**10**) (4 mg, 0.007 mmol) dissolved in THF-d_8 or C_6D_6 was added to a 5 mm thick-walled NMR tube fitted with a Teflon valve. The sample was subjected to three freeze-pump-thaw cycles and pressurized with 8 atm H_2. For C_6D_6: No amount of *trans*-$^{(tBu)4}$(PCP)Ir(CO)(H)$_2$ (**11**) was observed after 7 days at 100 °C. For THF: Upon heating the sample at 100 °C for 4 days, 41% conversion to *trans*-$^{(tBu)4}$(PCP)Ir(CO)(H)$_2$ (**11**) was observed. No change to the product ratio was observed after further heating for 3 more days.

*Reaction of $^{(tBu)4}$(PCP)Ir(CO) (**10**) with H_2 (1 atm, acid catalyzed).* [Hpyr]BF_4 (5 µL, 1 M in CH_3CN, 0.005 mmol) was added to an NMR tube fitted with a J. Young style Teflon valve and the solvent was removed under vacuum. $^{(tBu)4}$(PCP)Ir(CO) (**10**) (8 mg, 0.0013 mmol) was dissolved in THF-d_8 and added to the tube to give a yellow solution. The sample was subjected to three freeze-pump-thaw cycles and pressurized with 1 atm H_2. No color change was observed. After 30 minutes at room temperature, the solution was found to contain $^{(tBu)4}$(PCP)Ir(CO) (**10**) (10%), *trans*-$^{(tBu)4}$(PCP)Ir(CO)(H)$_2$ (**11**) (82%) and [$^{(tBu)4}$(PCP)Ir(CO)(H)(pyr)]BF_4 (**12**) (8%). After a further 2 days at room temperature the ratio remained unchanged, though H_2 was still observed in the ^{1}H NMR spectrum.

*Reaction of $^{(tBu)4}$(PCP)Ir(CO) (**10**) with H_2 (1 atm, acid catalyzed) quenched with base.* To a J. Young NMR tube containing $^{(tBu)4}$(PCP)Ir(CO) (**10**) (10%), *trans*-$^{(tBu)4}$(PCP)Ir(CO)(H)$_2$ (**11**) (82%) and [$^{(tBu)4}$(PCP)Ir(CO)(H)(pyr)]BF_4 (**12**) (8%) in THF-d_8, triethylamine (18 µL, 0.013 mmol) was added under a flow of hydrogen. ^{31}P NMR spectroscopy revealed complete conversion of [$^{(tBu)4}$(PCP)Ir(CO)(H)(pyr)]BF_4 (**12**) back to $^{(tBu)4}$(PCP)Ir(CO) (**10**) and the concentration of

trans-$^{(tBu)4}$(PCP)Ir(CO)(H)$_2$ (**11**) remained unchanged. No change in ratio was observed after the sample was submitted to three freeze-pump-thaw cycles.

*Reaction of $^{(tBu)4}$(PCP)Ir(CO) (**10**) with H_2 (8 atm, acid catalyzed with [Hpyr]BF_4).* [Hpyr]BF_4 (4 µL, 1 M in CH_3CN, 0.004 mmol) was added to a 5 mm thick-walled NMR tube fitted with a Teflon valve using a glass syringe. The solvent was removed *in vacuo* and $^{(tBu)4}$(PCP)Ir(CO) (**10**) (4 mg, 0.007 mmol) dissolved in THF-d_8 was added to the tube. The sample was subjected to three freeze-pump-thaw cycles and pressurized with 8 atm H_2. An immediate color change from yellow to colorless was observed. NMR spectroscopy revealed quantitative conversion to *trans*-$^{(tBu)4}$(PCP)Ir(CO)(H)$_2$ (**11**). Removal of H_2 atmosphere gave partial conversion back to $^{(tBu)4}$(PCP)Ir(CO) (**10**). *trans*-$^{(tBu)4}$(PCP)Ir(CO)(H)$_2$ (**11**). ^{1}H NMR (THF-d_8, 499.71 MHz): δ 6.77 (d, $^3J_{HH}$ = 7.6 Hz, 2H; Ar-*H*), 6.60 (t, $^3J_{HH}$ = 7.2 Hz, 1H; Ar-*H*), 3.43 (vt, $^2J_{PH}$ + $^4J_{PH}$ = 3.8 Hz, 4H; ArCH_2PR_2), 1.35 (vt, $^2J_{PH}$ + $^4J_{PH}$= 6.5 Hz, 36H; PC(CH_3)$_3$), -9.74 (t, $^2J_{PH}$ = 14 Hz, 2H; Ir-*H*). ^{31}P{^{1}H} NMR (THF-d_8, 202.31 MHz): δ 75.3 (s).

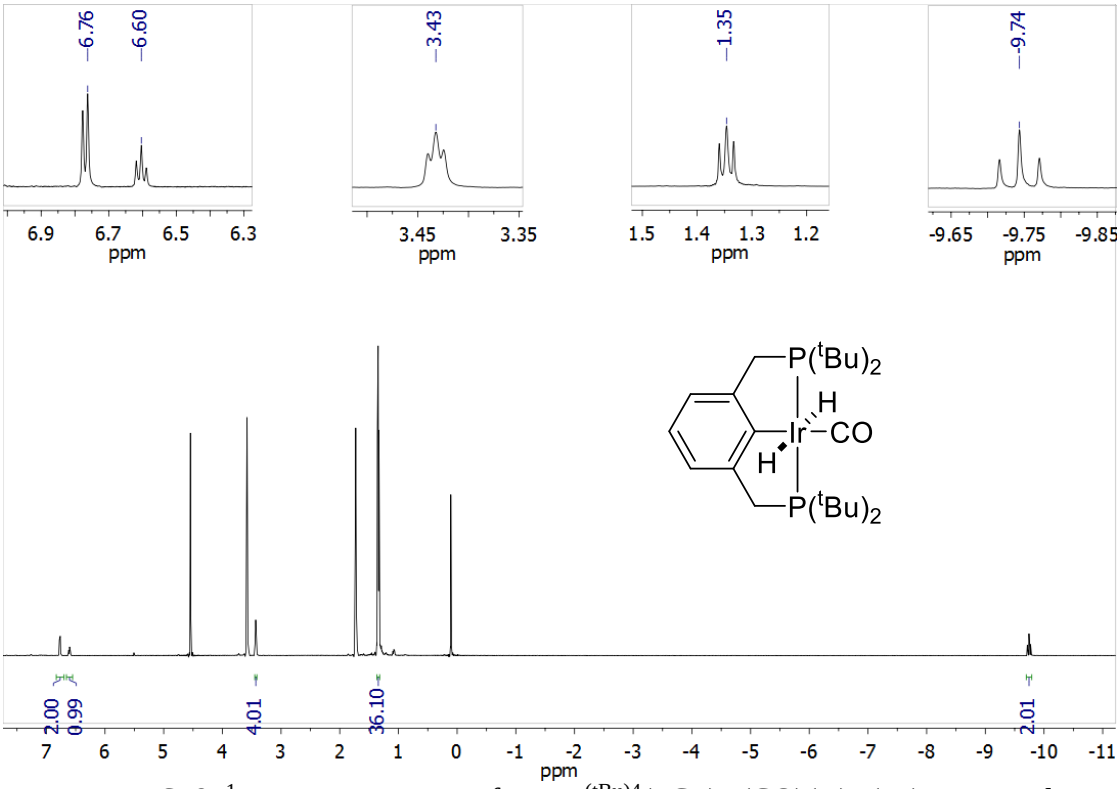

Figure S29. ^{1}H NMR spectrum of *trans*-$^{(tBu)4}$(PCP)Ir(CO)(H)$_2$ (**11**) in THF-d_8

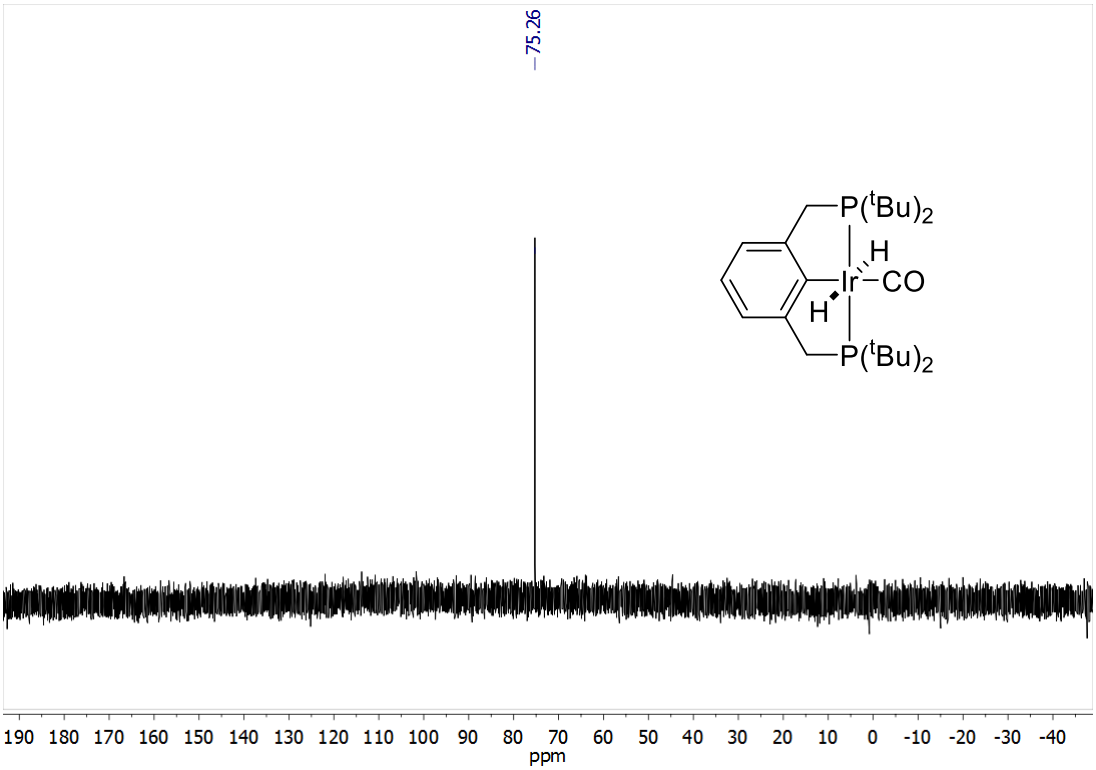

Figure S30. $^{31}P\{^{1}H\}$ NMR spectrum of *trans*-$^{(tBu)4}$(PCP)Ir(CO)$(H)_2$ (**11**) in THF-d_8

*Reaction of [$^{(tBu)4}$(PCP)Ir(CO)(H)(pyr)]BF_4 (**12**) with H_2.* [$^{(tBu)4}$(PCP)Ir(CO)(H)(pyr)]BF_4 (**12**) (3.5 mg, 0.004 mmol) was dissolved in THF-d_8 and added to a 5 mm thick-walled NMR tube fitted with a Teflon valve. The solution was freeze-pump-thawed three times and placed under 8 atm H_2. Quantitative conversion to *trans*-$^{(tBu)4}$(PCP)Ir(CO)$(H)_2$ (**11**) was observed by ^{1}H NMR and ^{31}P NMR spectroscopy.

*Reaction of $^{(iPr)4}$(PCP)Ir(CO) (**13**) with H_2 (8 atm, acid catalyzed with [Hpyr]BF_4).* [Hpyr]BF_4 (4 µL, 1 M in CH_3CN, 0.004 mmol) was added to a 5 mm thick-walled NMR tube fitted with a Teflon valve using a glass syringe. The solvent was removed *in vacuo* and $^{(iPr)4}$(PCP)Ir(CO) (**13**) (3.9 mg, 0.007 mmol) dissolved in THF-d_8 was added to the tube. The sample was subjected to three freeze-pump-thaw cycles and pressurized with 8 atm H_2. An immediate color change from yellow to colorless was observed. NMR spectroscopy revealed conversion to *trans*-$^{(iPr)4}$(PCP)Ir(CO)$(H)_2$ (**14**) and [$^{(iPr)4}$(PCP)Ir(CO)(H)(pyr)]BF_4 (**15**) (37:63). The ratio of products remained constant after mixing at room temperature for an additional 2 days. NMR data for **14** are consistent with previous reports.[4]

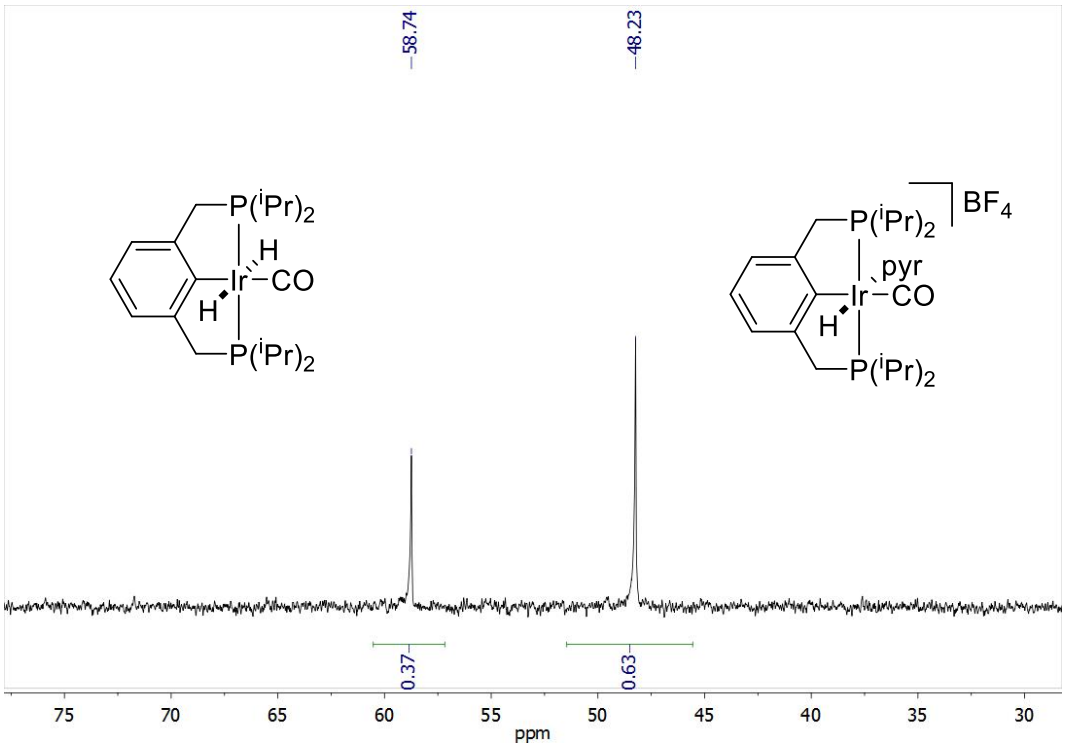

Figure S31 $^{31}P\{^{1}H\}$ NMR spectrum of $^{(iPr)4}$(PCP)Ir(CO) (**13**) and H_2 (8 atm) with [Hpyr]BF_4 in THF-d_8

pK_a Determination of [$^{(tBu)4}$(POCOP)Ir(CO)(H)]BArF$_{20}$ (3-BArF$_{20}$)

In a nitrogen-filled glovebox, 24.1 mg (0.0186 mmol) **3-BArF$_{20}$** was dissolved in a mixture of CD_2Cl_2 and CH_2Cl_2 (0.3 mL and 2 mL respectively) giving a yellow/orange solution. To this solution was added 1 equiv. *N*,*N*-dimethylaniline (100 μL of 0.19 M solution in CH_2Cl_2). Another 2 mL CH_2Cl_2 was added to ensure complete solubility of all species present; $^{(tBu)4}$(POCOP)Ir(CO) (**1**) has lower solubility than **3-BArF$_{20}$** in CH_2Cl_2. A 0.4 mL aliquot was taken from the solution and analyzed by ^{1}H and ^{31}P NMR spectroscopy. The same experiment was repeated with 1.1 equiv. *N*,*N*-dimethylaniline and similar results were obtained (*vide infra*).

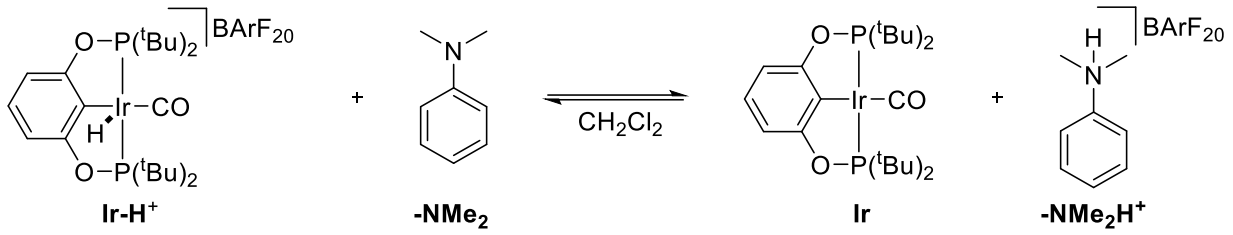

Ir-H$^+$ **-NMe$_2$** **Ir** **-NMe$_2$H$^+$**

1 equiv. **Ir-H$^+$** and 1 equiv. **–NMe$_2$**; ratios of each species at equilibrium by ^{1}H and ^{31}P NMR:

Ir-H$^+$ = 0.27 **-NMe$_2$** = 0.27 **Ir** = 0.73 **-NMe$_2$H$^+$** = 0.73

The ratios represented are the average of the ratios observed at 1 h and 24 h. There was minimal change in the ratios between 1 h and 24 h. There is an equilibrium between **–NMe$_2$** and **–NMe$_2$H$^+$**, thus only 1 set of signals is observed by ^{1}H NMR for the weighted average of the two species;[5] when integrated versus the total ^{t}Bu protons for **Ir** and **Ir-H$^+$**, the integration of **–NMe$_2$**/**-NMe$_2$H$^+$** represents 1 equiv. The ratios of **Ir** and **Ir-H$^+$** at equilibrium were experimentally determined by integrating the ^{31}P NMR spectra; they were the only ^{31}P containing species present. Characteristic ^{1}H NMR aromatic signals for **Ir** and **Ir-H$^+$** were also integrated and the ratios obtained were in line with those from the ^{31}P NMR spectra. The ratio of **–NMe$_2$** present at equilibrium was determined by subtracting the ratio of **Ir** from the number of equivalents of **–NMe$_2$** initially added. The ratio of **–NMe$_2$H$^+$** should be equal to that of **Ir**. The experimentally determined pK_a^{THF}(**-NMe$_2$H$^+$**) is 4.9.[6] It has been previously been shown that for metal-hydride complexes, pK_a^{THF} ≈ pK_a^{CH2Cl2}.[7]

The ratio of each species at equilibrium was substituted into the following equilibrium expression:

$$K = \frac{[\mathrm{Ir}][-\mathrm{NMe_2H^+}]}{[\mathrm{Ir-H^+}][-\mathrm{NMe_2}]} = \frac{(0.73)^2}{(0.27)^2} = 7.31$$

The pK_a of **Ir-H$^+$** was obtained by referencing versus the known pK_a of **–NMe$_2$H$^+$** in the following equation:[8]

pK_a(**Ir-H$^+$**) = pK_a(**-NMe$_2$H$^+$**) – log$K$

pK_a(**Ir-H$^+$**) = 4.9 – log(7.31) = 4.0

The analogous calculation was performed when 1.1 equiv. *N*,*N*-dimethylaniline was used and a pK_a of 4.0 was also obtained. Therefore, pK_a^{CH2Cl2}(**Ir-H$^+$**) = 4.0 ± 0.1.

Solubility Observations from pK_a Studies

Studies of the pK_a values for **3-BF$_4$** showed that limited solubility of salts could give misleading results. When deprotonation of **3-BF$_4$** was screened with a series of bases, solid precipitates formed even in the presence of weak bases. Once the more soluble **3-BArF$_{20}$** was studied for deprotonation, there was no driving force for salt formation. Pyridine was not a suitable base for deprotonation, since it coordinated as a sixth ligand to an unsaturated Ir center to give **8**. When **1** was reacted with [Hpyr]BF_4 in CD_2Cl_2, protonation was not obtained, likely due to the limited solubility of [Hpyr]BF_4 and the corresponding Ir(III) adduct. Protonation of **1** with pyridinium is complicated by the complexation of pyridine. While pyridine is a better base than **1** based on the experimentally determined pK_a of **3-BArF$_{20}$** and a simple acid-base reaction would not be expected, formation of **8** is observed. This is likely due to formation of a soluble octahedral Ir(III) compound where pyridine can stabilize an unsaturated Ir(III) metal center. Further support for the competition of an acid-base reaction versus stabilization of an unsaturated metal center was found when **3-BArF$_{20}$** was completely deprotonated by the non-coordinating base 2,6-lutidine rather than coordination of the lutidine moiety in the sixth coordination site. In this case, deprotonation is favored over coordination of a sixth ligand since 2,6-lutidine is sterically hindered.

Hydrogen Pressurization System[9]

Assembly of High Pressure Setup

Figure S32 is an illustration of the complete hydrogen delivery system. 3/8" Copper tubing was connected to the H_2 regulator with a compression fitting. A coil was placed in the copper tubing to allow for flexibility. The majority of joints were connected by soldering with 3/8" copper tees and 7/8" couplings. 90° joints in copper tubing were achieved by use of compression fittings and Teflon tape to seal the joint. Two needle valves were fitted to the apparatus. One valve is for connecting to a Schlenk line if reduced pressure is necessary. The other needle valve connects to an oil bubbler for purging, checking for leaks, and venting the system. Currently, our system is fitted with a 100 psig (max) pressure gauge, however any gauge with an NPT (national pipe thread) fitting is suitable. If higher pressures are desired, accommodations must be made as current needle valves are only rated to 150 psi.

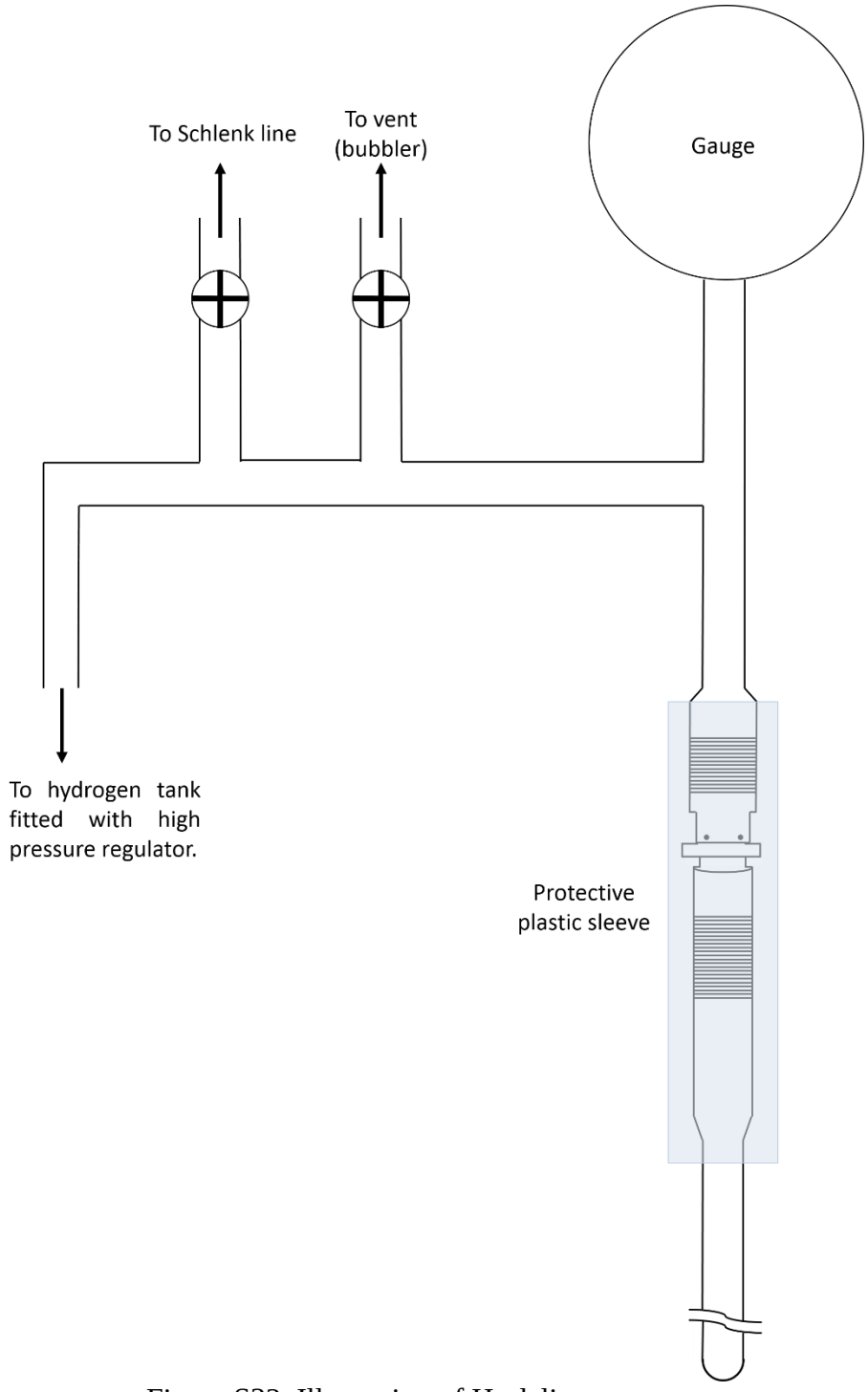

Figure S32. Illustration of H_2 delivery system.

Due to the "right-handed" threading of the glass and Teflon pin, the connection of the Teflon pin to the brass fitting is important (Figure S33). To prevent loosening the Teflon cap from the brass fitting while attaching and detaching the tube, set screws are used to secure the cap in place. The Teflon pins have been modified after purchase to accommodate the pressurization system. To prevent opening the seal between the glass and Teflon pin while removing the tube

from the system, grooves were cut into the Teflon pin. A custom wrench made to fit the grooves is used to loosen only the cap from the brass system. This results in removal of the NMR tube without releasing any pressure.

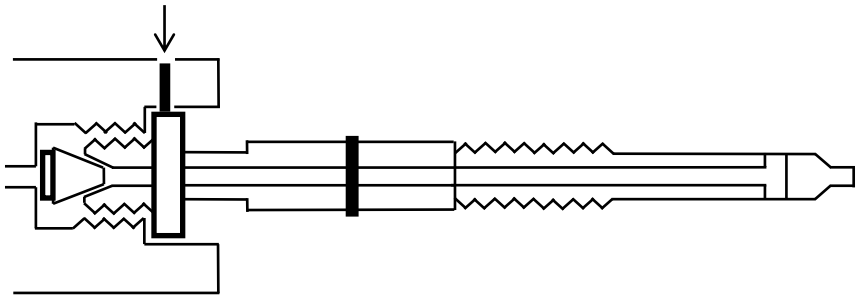

Figure S33. Depiction of Teflon fitting for high pressure tubes while attached to the H_2 system. Arrow indicates placement of setscrew to hold Teflon fitting in place. Another setscrew is placed 90° from the indicated setscrew.

How to Pressurize an NMR Tube

Caution: **Hydrogen is an extremely flammable gas. Remove all open flames while system is in use. While dealing with high pressures, use all safety precautions including but not limited to Kevlar gloves and sleeves, lab coat, facemask, and blast shields. Do not operate system while alone. While transporting tubes, secondary, shatter-proof containment should always be used.**

The NMR sample is degassed by three freeze-pump-thaw cycles by screwing the NMR tube into the custom attachment made to fit a Schlenk line (Figure S34). After the sample has been degassed it is ready for pressurization. Twist the tube into the open end of the apparatus (finger tight). Using the custom wrench, tighten the Teflon pin into the brass fitting using the customized grooves and turn clockwise (Figure S35 and S36; caution, over tightening the cap at this point can lead to disfiguration of the Teflon pin at the threading as well as the customized groove). With the small allen wrench, tighten both set screws into place (*vide infra*, Figure S40). The Teflon pin should be secured and leak free. Raise the plastic protective sleeve around the tube and screw on completely (*vide infra*, Figure S38).

Figure S34. From left to right: i) Brass custom piece to fit tubes to Schlenk Line. ii) Top of piece. A small valve for gas and vacuum flow. iii) Bottom of piece. Threading to match Teflon pin and Teflon ferrule to ensure a tight seal to tube. iv) Teflon ferrule. This is affixed to the brass piece with a silicon based sealant.

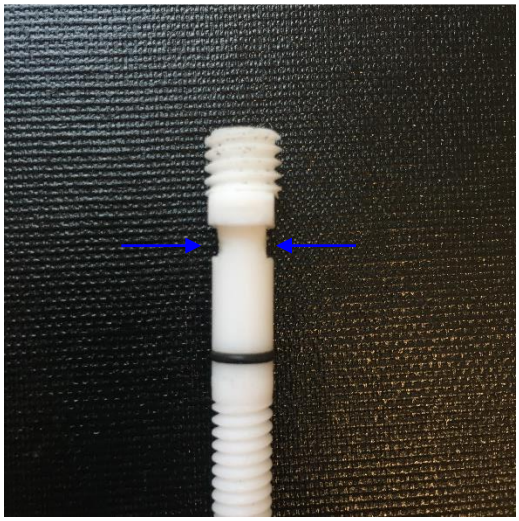

Figure S35. Teflon pin after modification. Modification highlighted with blue arrows.

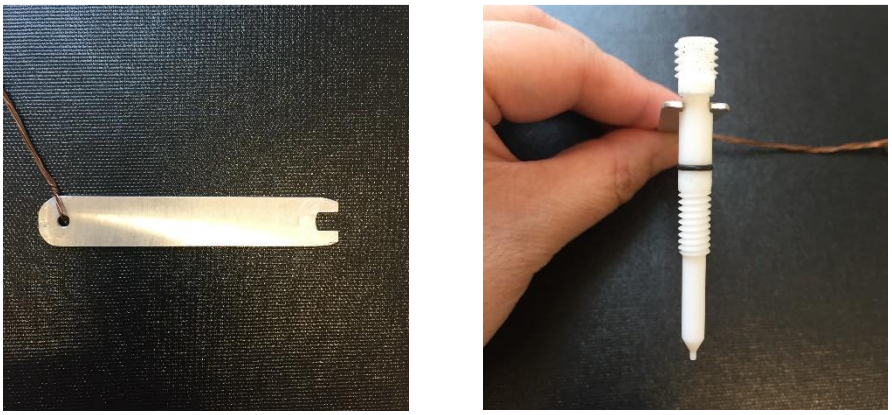

Figure S36. Left: Customized wrench for securing and removing NMR tube from system. Right: Wrench positioned in customized grooves on Teflon pin.

With the vacuum needle valve closed and the vent valve open, turn on the hydrogen tank and achieve a moderate flow of hydrogen. Purge the system for approximately 15 minutes. After venting is finished, close the vent valve and carefully raise the pressure to 20 psig. Ensure that the gauge on the pressurization system and the secondary gauge on the regulator are reading the same value. While pressurizing, leaks are more likely to occur from the needle valve, this can be identified by bubbles in the oil. Tighten the needle valve if necessary. Once the system has been checked, the tube can be opened by twisting the neck of the tube (under the plastic protective sleeve) counter-clockwise. With the tube open, raise the pressure delivered from the regulator by controlling the diaphragm to the desired pressure. Once achieved, close the tube by twisting the tube clockwise. Close the H_2 tank at the main valve, ensuring to leave the needle valve on the

regulator open. Slowly open the vent valve and release the pressure in the system. Once the pressure is released, close the needle valve on the regulator. Remove the plastic safety sleeve from the system and loosen the allen screws. Using the wrench, carefully remove the tube by twisting counter-clockwise. Place the tube in secondary containment.

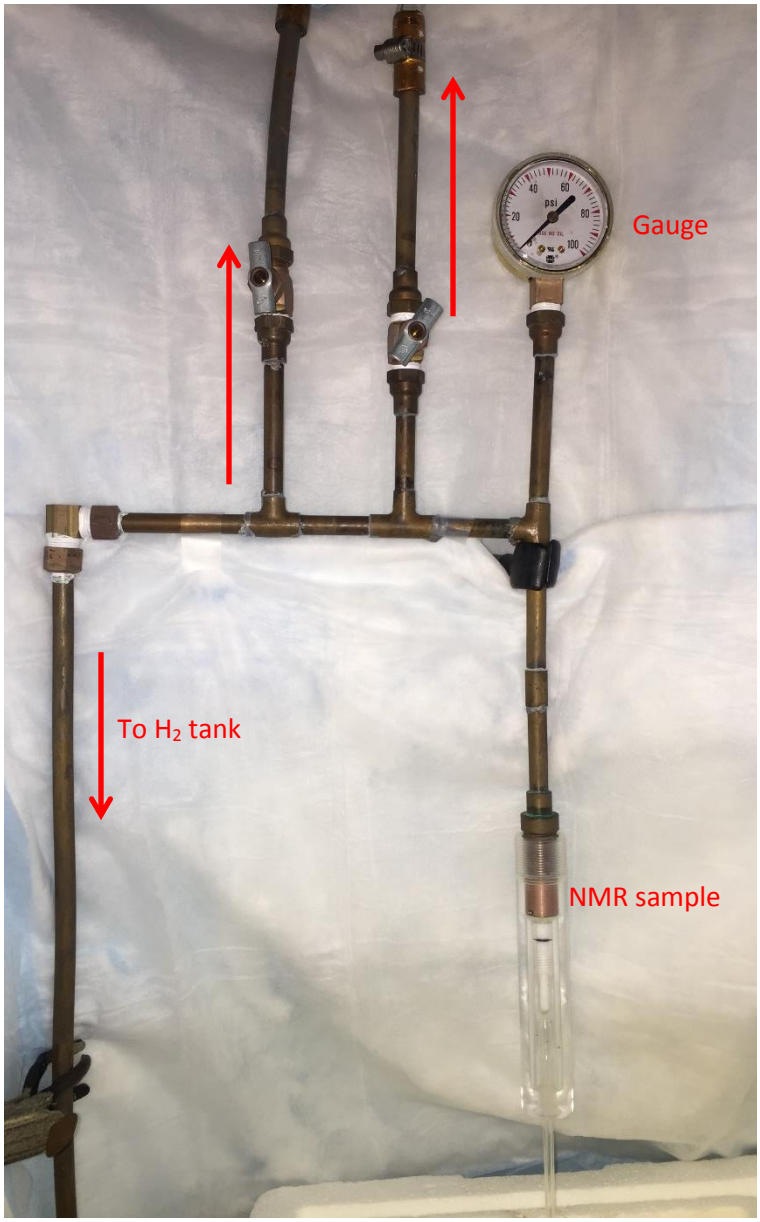

Figure S37. H_2 delivery system.

Figure S38. Close-up of sample attachment to apparatus.

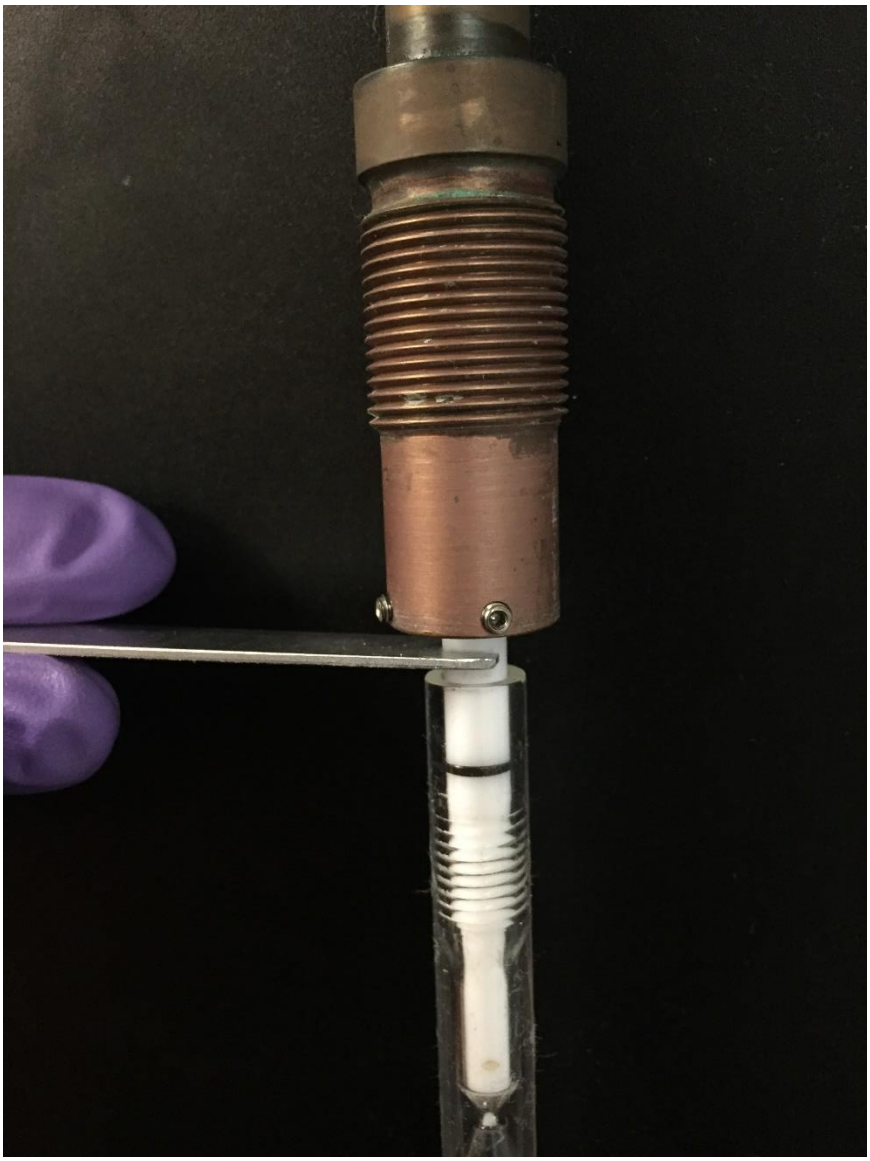

Figure S39. Using the custom wrench to tighten sample to copper fitting on H_2 apparatus. It is especially important to use the custom wrench when removing the sample to prevent venting the pressure in the sample.

Figure S40. Tightening one of two set screws to secure Teflon pin. By tightening the set screws, the Teflon cap will not be loosened while manipulating sample during pressurization.

Figure S41. Both set screws tightened. The sample is ready for the plastic protective sleeve.

Part Numbers

The following parts were used to assemble the custom-made pressurization system:

3/8” copper piping
3/8” compression fittings
3/8” copper tees, couplings, and elbows
1/4” NPT fittings

Wilmad-LabGlass:

522-PV-7	5 mm heavy wall precision pressure/vacuum valve NMR sample tube 7" L, 500MHz
OF-70	Polytetrafluoroethylene (PTFE) stepped cone ferrule
PV-ANV	Needle valve
PV-ANV-O	O-Ring for needle valve

VWR (USA):

55850-275	VWR Heavy-duty single-stage gas regulator Delivery pressure: 600 psig; Supply pressure: 4,000 psig
300007-378	Welding and compressed gas gauge, Ametek U.S. gauge

Grainger:

1VPW3	Needle valve, straight, brass, ¼ in., MNPT Maximum pressure limit of 150 psi

X-ray Crystallography

X-ray diffraction experiments were carried out on a Bruker APEX II single crystal X-ray diffractometer using Mo-radiation (λ = 0.71073Å) at -173 ºC. The crystals were mounted on loops with immersion oil. The data was integrated and scaled using SAINT, SADABS within the APEX2 software package by Bruker.[10] Structures ***trans*-5** and **7-BF_4** were solved by direct methods (SHELXS, SIR97[11]) producing a complete heavy atom phasing model consistent with the proposed structure. The structures were completed by difference Fourier synthesis with SHELXL97.[12] Scattering factors are from Waasmair and Kirfel.[13] Using Olex2,[14] structures **12** and **[$^{(iPr)4}$(PCP)Ir]$_2$(μ-N_2)** were solved with the XS[15] structure solution program using direct or Patterson methods and refined with the XL[15] refinement package using least squares minimization. The non-hydrogen atoms were refined anisotropically. Hydrogen atoms were refined using the riding model.

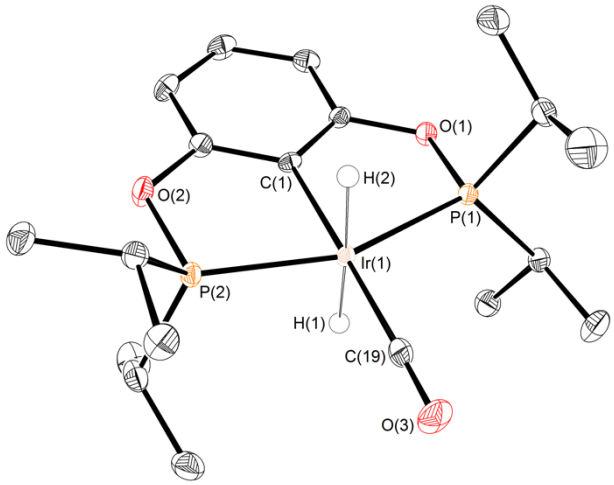

Figure S42. ORTEP[16] of ***trans*-5** shown with thermal ellipsoids at 50% probability. Hydrogen atoms, except for the Ir-bound hydrides, are omitted for clarity. Selected bond lengths (Å) and angles (°) for *trans*-$^{(iPr)4}$(POCOP)Ir(CO)$(H)_2$ (***trans*-5**): Ir(1)-C(1) 2.0614(16), Ir(1)-P(1) 2.2894(4), Ir(1)-P(2) 2.2815(4), Ir(1)-C(19) 1.8945(18), C(19)-O(3) 1.145(2); C(19)-Ir(1)-C(1) 178.80(7), C(1)-Ir(1)-P(1) 78.52(5), C(1)-Ir(1)-P(2) 78.66(5), P(1)-Ir(1)-P(2) 157.14(2).

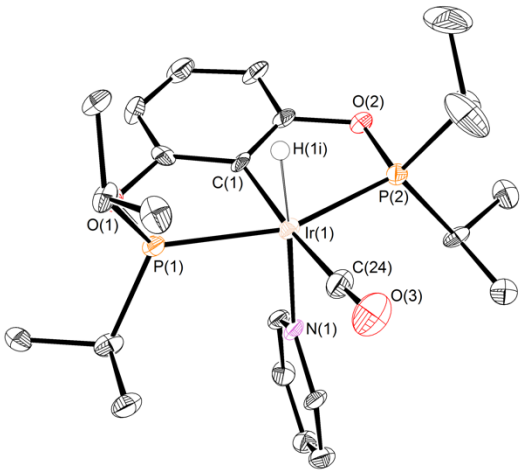

Figure S43. ORTEP[16] of **7-BF_4** shown with thermal ellipsoids at 50% probability. BF_4 anion and hydrogen atoms, except for the Ir-bound hydride, are omitted for clarity. Selected bond lengths (Å) and angles (°) for [$^{(iPr)4}$(POCOP)Ir(CO)(H)(pyr)]BF_4 (**7-BF_4**): Ir(1)-C(1) 2.040(8), Ir(1)-P(1) 2.319(2), Ir(1)-P(2) 2.320(2), Ir(1)-N(1) 2.236(6), Ir(1)-C(24) 1.927(8), C(24)-O(3) 1.142(9); C(24)-Ir(1)-N(1) 95.2(3), C(1)-Ir(1)-N(1) 93.3(3), N(1)-Ir(1)-P(1) 93.4(2), N(1)-Ir(1)-P(2) 92.6(2).

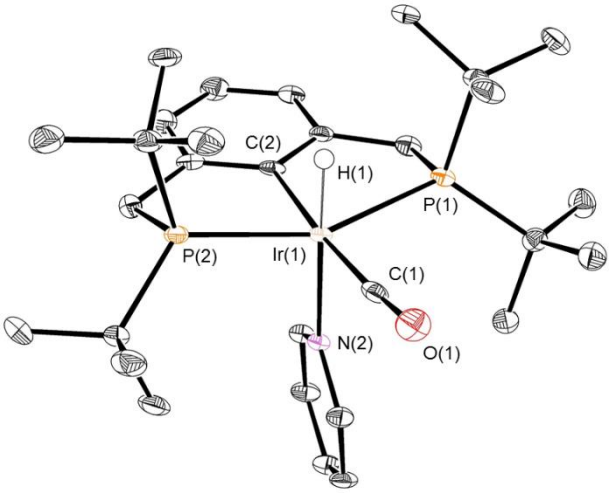

Figure S44. ORTEP[16] of **12** shown with thermal ellipsoids at 50% probability. BF_4 anion, solvent of crystallization (CH_2Cl_2) and hydrogen atoms, except for the Ir-bound hydride, are omitted for clarity. There were two molecules in the asymmetric unit, only fragment one is shown. Selected bond lengths (Å) and angles (°) for [$^{(tBu)4}$(PCP)Ir(CO)(H)(pyr)]BF_4 (**12**): Ir(1)-C(2) 2.103(4), Ir(1)-P(1) 2.363(1), Ir(1)-P(2) 2.365(1), Ir(1)-N(2) 2.234(3), Ir(1)-C(1) 1.918(4), C(1)-O(2) 1.138(5), P(1)-Ir(1)-P(2) 156.12(4), P(1)-Ir(1)-N(2) 97.57(8), P(2)-Ir(1)-N(2) 99.12(8), C(2)-Ir(1)-N(2) 88.7(1), C(1)-Ir(1)-N(2) 95.4(2).

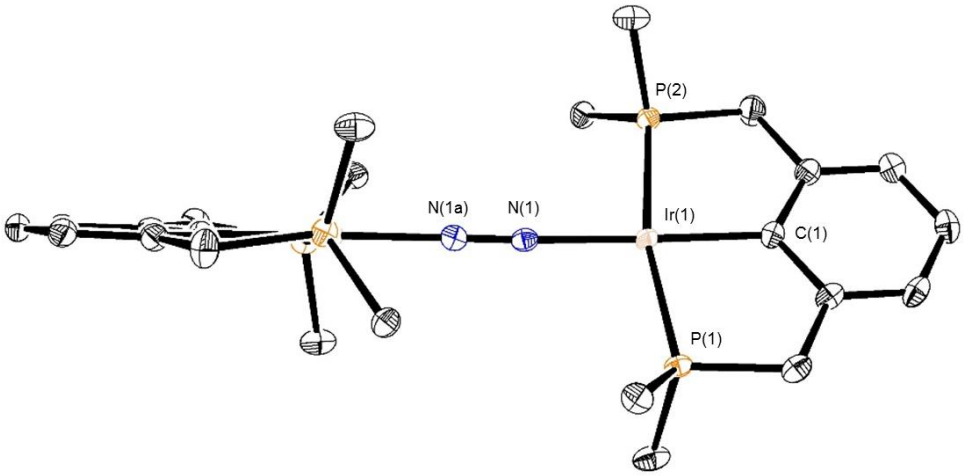

Figure S45. ORTEP[16] of **[$^{(iPr)4}$(PCP)Ir]$_2$(μ-N_2)** shown with thermal ellipsoids at 50% probability. ^{i}Pr groups are truncated and hydrogen atoms are omitted for clarity. A crystallographic mirror plane bisects the N-N bond. Selected bond lengths (Å) and angles (°) for **[$^{(iPr)4}$(PCP)Ir]$_2$(μ-N_2):** Ir(1)-C(1) 2.041(3), Ir(1)-P(1) 2.2687(7), Ir(1)-P(2) 2.2684(7), Ir(1)-N(1) 1.950(2), N(1)-N(1a) 1.125(3), P(1)-Ir(1)-P(2) 166.15(3), C(1)-Ir(1)-N(1) 177.93(10).

Table S1. Crystallographic data for complexes ***trans*-5**, **7-BF_4**, **12**, and **$[^{(iPr)4}$(PCP)Ir]$_2$(μ-N_2)**.

	***trans*-5**	**7-BF_4**	**12**	**$[^{(iPr)4}$(PCP)Ir]$_2$(μ-N_2)**
Empirical formula	$C_{19}H_{33}IrO_3P_2$	$C_{24}H_{37}BF_4IrNO_3P_2$	$C_{62}H_{102}B_2Cl_4F_8Ir_2N_2O_2P_4$	$C_{40}H_{70}Ir_2N_2P_4$
Formula weight	563.59	728.49	1731.15	1087.26
Temperature (K)	100(2)	100(2)	100(2)	100(2)
Wavelength (Å)	0.71073	0.71073	0.71073	0.71073
Crystal system	Triclinic	Triclinic	Triclinic	Monoclinic
Space group	P -1	P -1	P -1	C2/c
Unit cell axes (Å)	a = 7.8388(5) b = 9.9117(7) c = 15.1225(10)	a = 10.7054(9) b = 14.1797(10) c = 18.4651(16)	a = 12.9175(9) b = 14.7329(10) c = 20.1421(14)	a = 21.4680(15) b = 10.9382(6) c = 20.3858(14)
Unit cell angles (°)	α = 105.935(3) β = 92.176(3) γ = 107.411(3)	α = 89.544(4) β = 88.624(4) γ = 88.014(3)	α = 109.001(4) β = 96.628(4) γ = 90.772(4)	α = 90 β = 111.938(5) γ = 90
Volume (Å^3)	1068.76(12)	2800.4(4)	3594.9(4)	4440.4(5)
Z	2	4	2	4
Density (calculated) (Mg/m^3)	1.751	1.728	1.599	1.626
Absorption coefficient (mm^{-1})	6.411	4.935	3.998	6.160
F(000)	556	1440	1736.0	2152.0
Crystal size (mm^3)	0.18 × 0.15 × 0.10	0.16 × 0.13 × 0.020	0.4 × 0.3 × 0.03	0.04 × 0.03 × 0.01
Theta range for data collection	2.26 to 28.42°	1.437 to 28.342°	2.928 to 56.87°	4.09 to 56.808°
Index Ranges	-10 ≤ h ≤ 10 -13 ≤ k ≤ 13 -20 ≤ l ≤ 20	-14 ≤ h ≤ 14 -18 ≤ k ≤ 18 0 ≤ l ≤ 24	-17 ≤ h ≤ 17 -19 ≤ k ≤ 19 -26 ≤ l ≤ 26	-28 ≤ h ≤ 28 -14 ≤ k ≤ 14 -27 ≤ l ≤ 27
Reflections collected	46232	70125	156408	97720
Independent reflections	5353	13356	17805	5567
R_{int}	0.0274	0.0778	0.0693	0.0531
Data / restraints / parameters	5353 / 0 / 242	13356 / 25 / 672	17805 / 1 / 807	5567 / 0 / 225
Goodness-of-fit on F^2	1.045	1.016	1.032	1.039
Final R indices [I>2σ(I)]	R_1 = 0.0132, wR_2 = 0.0268	R_1 = 0.0494, wR_2 = 0.1201	R_1 = 0.0344, wR_2 = 0.0726	R_1 = 0.0190, wR_2 = 0.0374
R indices (all data)	R_1 = 0.0143, wR_2 = 0.0271	R_1 = 0.0756, wR_2 = 0.1358	R_1 = 0.0545, wR_2 = 0.0820	R_1 = 0.0286, wR_2 = 0.0405
Largest diff. peak and hole (e. Å^{-3})	0.558 and -0.560	3.090 and -2.688	2.33 and -2.14	1.28 and -0.79

References

[1] Göttker-Schnetmann, I.; White, P. S.; Brookhart, M. *Organometallics* **2004**, *23*, 1766–1776.
[2] Goldberg, J. M.; Wong, G. W.; Brastow, K. E.; Kaminsky, W.; Goldberg, K. I.; Heinekey, D. M. *Organometallics* **2015**, *34*, 753-762.
[3] Grönberg, K. L. C.; Henderson, R. A.; Oglieve, K. E. *J. Chem. Soc., Dalton Trans.* **1998**, 3093–3104.
[4] Rybtchinski, B.; Ben-David, Y.; Milstein, D. *Organometallics* **1997**, *16*, 3786-3793.
[5] Drago, R. S., Physical Methods for Chemists. 2nd ed.; Surfside Scientific Publishers: Gainesville, Fl, 1992.
[6] Kaljurand, I.; Kütt, A.; Sooväli, L.; Rodima, T.; Mäemets, V.; Leito, I.; Koppel, I. A. *J. Org. Chem.* **2005**, *70*, 1019–1028.
[7] (a) Jia, G.; Lau, C.-P. *Coord. Chem. Rev.* **1999**, *190-192*, 83–108. (b) Li, T.; Lough, A. J.; Morris, R. H. *Chem. Eur. J.* **2007**, *13*, 3796–3803.
[8] Saouma, C. T.; Kaminsky, W.; Mayer, J. M. *J. Am. Chem. Soc.* **2012**, *134*, 7293-7296.
[9] Adapted from: Cherry, S. D. T. Ph. D. Dissertation, University of Washington, Seattle, WA, 2016.
[10] Bruker APEX2 (Version 2.1-4), SAINT (version 7.34A), SADABS (version 2007/4), BrukerAXS Inc, Madison, Wisconsin, USA, 2007.
[11] (a) Altomare, A.; Burla, C.; Camalli, M.; Cascarano, G. L.; Giacovazzo, C.; Guagliardi, A.; Moliterni, A. G. G.; Polidori, G.; Spagna, R. SIR97: a new tool for crystal structure determination and refinement *J. Appl. Cryst.* **1999**, *32*, 115-119. (b) Altomare, A.; Cascarano, G. L.; Giacovazzo, C.; Guagliardi, A. Completion and refinement of crystal structures with SIR 92. *J. Appl. Cryst.* **1993**, *26*, 343-350.
[12] (a) Sheldrick, G. M. SHELXL-97, Program for the Refinement of Crystal Structures. University of Göttingen, Germany, 1997. (b) Mackay, S.; Edwards, C.; Henderson, A.; Gilmore, C.; Stewart, N.; Shankland, K.; Donald, A. *MaXus: a computer program for the solution and refinement of crystal structures from diffraction data*. University of Glasgow, Scotland, 1997.
[13] Waasmaier, D.; Kirfel, A. New Analytical Scattering Factor Functions for Free Atoms and Ions. *Acta Crystallogr., Sect. A* **1995**, *51*, 416-430.
[14] Dolomanov, O. V.; Bourhis, L. J.; Gildea, R. J.; Howard, J. A. K.; Puschmann, H. "OLEX2: a complete structure solution, refinement and analysis program." *J. Appl. Cryst.* **2009**, *42*, 339- 341.
[15] Sheldrick, G. M. *Acta Crystallogr. Sect. A* **2008**, *64*, 112-122.
[16] (a) Farrugia, L. J. *J. Appl. Cryst.* **2012**, *45*, 849-854. (b) Farrugia, L. J. *J. Appl. Cryst.* **1997**, *30*, 565.